HHS Public Access

Author manuscript

Cell Rep. Author manuscript; available in PMC 2022 December 10.

Published in final edited form as:

Cell Rep. 2022 November 15; 41(7): 111643. doi:10.1016/j.celrep.2022.111643.

Hippocampal parvalbumin interneurons play a critical role in memory development

Janelle M. Miranda[1], **Emmanuel Cruz**[1], **Benjamin Bessières**[1], **Cristina M. Alberini**[1,2,*]

[1]Center for Neural Science, New York University, 4 Washington Place, New York, NY 10003, USA

[2]Lead contact

SUMMARY

Episodic memories formed in early childhood rapidly decay, but their latent traces remain stored long term. These memories require the dorsal hippocampus (dHPC) and seem to undergo a developmental critical period. It remains to be determined whether the maturation of parvalbumin interneurons (PVIs), a major mechanism of critical periods, contributes to memory development. Here, we show that episodic infantile learning significantly increases the levels of parvalbumin in the dHPC 48 h after training. Chemogenetic inhibition of PVIs before learning indicated that these neurons are required for infantile memory formation. A bilateral dHPC injection of the γ-aminobutyric acid type A receptor agonist diazepam after training elicited long-term memory expression in infant rats, although direct PVI chemogenetic activation had no effect. Finally, PVI activity was required for brain-derived neurotrophic factor (BDNF)-dependent maturation of memory competence, i.e., adult-like long-term memory expression. Thus, dHPC PVIs are critical for the formation of infantile memories and for memory development.

In brief

Miranda et al. report that the levels of parvalbumin increase in the hippocampus of infant rats following learning and that hippocampal PV interneurons (PVIs) are required for the formation and storage of long-term infantile memory. Furthermore, PVIs are critical contributors of memory maturation promoted by BDNF.

Graphical Abstract

*Correspondence: ca60@nyu.edu.

AUTHOR CONTRIBUTIONS

C.M.A. and J.M.M. designed the experiments. J.M.M. performed the experiments and data analysis with the supervision of E.C., B.B., and C.M.A. All authors assisted with data interpretation. C.M.A. and J.M.M. wrote the manuscript with input from all authors.

DECLARATION OF INTERESTS

The authors declare no competing interests.

SUPPLEMENTAL INFORMATION

Supplemental information can be found online at https://doi.org/10.1016/j.celrep.2022.111643.

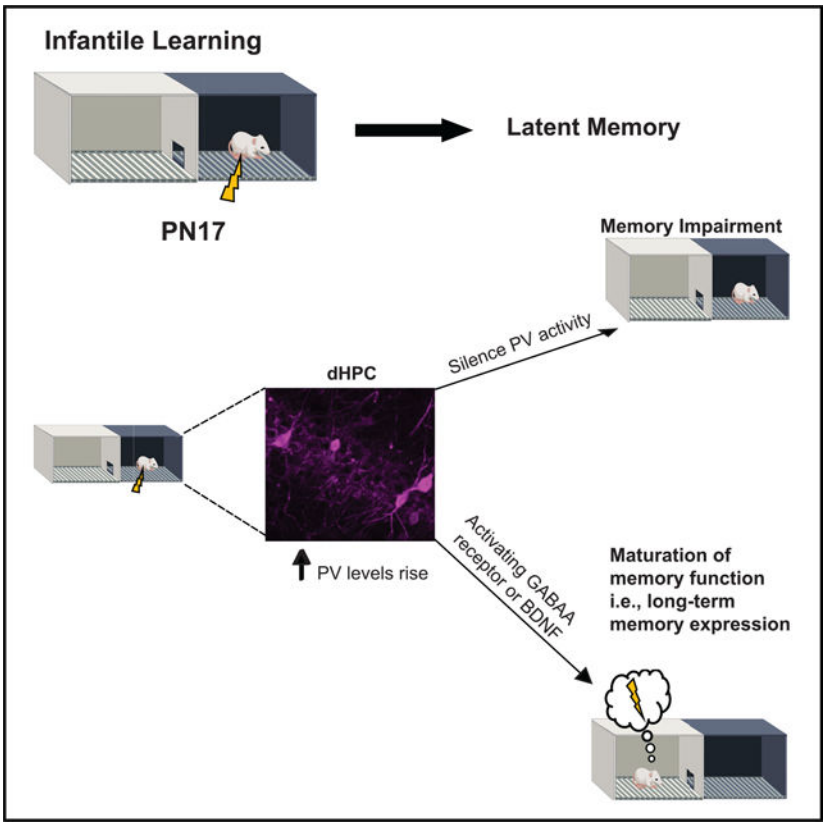

INTRODUCTION

In rodents as in humans, episodic infantile memories appear to be rapidly forgotten (Hartshorn et al., 1998; Hayne, 2004; Rovee-Collier and Cuevas, 2009; Campbell and Spear, 1972; Hartshorn et al., 1998; Li et al., 2014). This rapid forgetting is believed to explain infantile amnesia, the inability of adults to remember infantile experiences (Nadel and Zola-Morgan, 1984; Howes et al., 1993; Peterson et al., 2005; Mullally and Maguire, 2014).

Previous studies in rats and mice showed that memories formed during the infantile period are only apparently forgotten; in fact, they can reemerge later in life upon experiencing behavioral reminders or neuronal stimulation of cellular networks activated and tagged during infantile learning (Travaglia et al., 2016a; Guskjolen et al., 2018; Bessières et al., 2020). Contrary to what was previously believed, the formation of episodic infantile memories requires the hippocampus (Travaglia et al., 2016a), where mGluR5-dependent and brain-derived neurotrophic factor (BDNF)-dependent switch in the expression of the NMDA receptor subunits from a higher ratio of GluN2B/2A to the inverse plays a critical role (Travaglia et al., 2016a). These mechanisms had been discovered as important contributors of sensory systems' critical periods, particularly for the visual system (Quinlan et al., 1999; Carmignoto and Vicini, 1992), and the development of long-term potentiation in the hippocampus (Bellone and Nicoll, 2007).

Critical periods are temporal windows during which environmental stimuli are crucial for the proper development of brain functions (Hensch, 2005); their biological bases have been investigated mostly in the visual system, where, in addition to the mGluR5-dependent NMDA subunit switch and other molecular mechanisms, the maturation of inhibitory interneurons expressing the calcium-binding protein parvalbumins (PVIs) emerged as an important mechanism (Hensch, 2005).

PVIs are fast-spiking cells that exert most of their inhibitory influence via somatic synapses containing the alpha1 subunit of γ-aminobutyric acid A (GABAA) receptors (Klausberger et al., 2002; Fagiolini et al., 2004; Hensch, 2005). They form an inter-connected network capable of providing feedforward, feedback, and lateral inhibition to nearby pyramidal cells and generate gamma oscillations associated with critical period plasticity (Hensch, 2005; Hu et al., 2014; Reh et al., 2020). The development of PVIs is sensitive to experience and involves cell-extrinsic factors such as orthodenticle homeobox 2 (otx2) and BDNF, two mechanisms intimately associated with critical periods (Bozzi et al., 1995; Takesian and Hensch, 2013; Reh et al., 2020). In fact, in the mouse visual cortex, the maturation of inhibition and PVIs during the critical period is controlled by BDNF (Huang et al., 1999; Hanover et al., 1999; Takesian and Hensch, 2013), as overexpression of BDNF results in an accelerated maturation of visual acuity, hence the accelerated closure of the critical period (Huang et al., 1999; Hanover et al., 1999). Furthermore, the plasticity associated with critical periods follows the temporal development of parvalbumin (PV) circuits (Condé et al., 1996), and, in monkey, the hierarchical development of the visual cortex is paralleled by the maturation of PV-immunoreactive neurons (Condé et al., 1996). All these findings provide converging evidence that PVIs are key cellular players in critical periods and the developmental maturation of vision.

In our previous studies on infantile episodic memories in rats, we showed that, as for the functional maturation effect of BDNF on the visual system, administration of BDNF into the rat dorsal hippocampus (dHPC) at the time of inhibitory avoidance (IA) learning in infant rats (at postnatal day 17 [PN17]) is sufficient to accelerate the development of memory functions; i.e., the ability to express memory long term as in adults (Travaglia et al., 2016a). Studies in adult rodents have shown that PV is upregulated following contextual or spatial learning in the hippocampus, where PVIs play a critical role in long-term memory formation (Donato et al., 2013, 2015; Xia et al., 2017; Ognjanovski et al., 2017). However, whether PVIs are important for the functional maturation of hippocampus-dependent memories, i.e., long-term memory expression, remains to be determined. It also remains to be understood whether the ability of BDNF to accelerate the maturation of hippocampus-dependent memory functions involves hippocampal PVIs. Here we set out to address these questions by employing the aversive episodic learning task IA in rats and LE-Tg(Pvalb-iCre)2Ottc transgenic rats, which express Cre recombinase under the PV promoter, in combination with molecular and cellular investigations. We show that PVIs are necessary for the development of infantile memories and for BDNF’s ability to mature memory competence in infant rats.

RESULTS

Infantile learning significantly increases PV levels in the dHPC

The levels of PV mRNA and protein are known to increase over developmental ages in several brain regions, including the hippocampus, visual cortex, somatosensory cortex, and cingulate cortex (de Lecea et al., 1995; Seto-Ohshima et al., 1990; Que et al., 2021). Here we employed western blot analyses to assess PV levels in the dHPC of infant (PN17), juvenile (PN24), and young adult (PN80) rats and found, in agreement with those previous studies, that the level of PV significantly increases between PN17 and PN24 but does not further change between PN24 and PN80 (Figure 1A).

We then focused on PN17 infant rats to determine whether the level of PV in their dHPC changes following episodic learning. We performed a time course analysis following IA training using western blots on dHPC extracts obtained at 30 minutes (min), 9 hours (h), 24 h, and 48 h post training and compared them with extracts obtained from dHPC of untrained rats (hereafter referred to as naive controls). As shown in Figure 1B, PV levels gradually rose over time following training relative to naive controls euthanized at matched time points and resulted in a significant increase at 48 h after training. This increase was the result of associative learning, as no change in PV level was detected in the dHPC of rats at PN19 after receiving, at PN17, a footshock immediately after being placed on a grid (shock only [SO]) (Figure 1B), a protocol that does not elicit an associative IA memory and controls for the effects of the footshock (Travaglia et al., 2016a). Additionally, PV levels did not significantly change in the dHPC over developmental ages of PN17 and PN19 (Figure S1), suggesting that the post-training increase was indeed associated with IA learning.

The time-course analysis was then extended to other markers of inhibitory cells or mechanisms and particularly to gephyrin and vesicular GABA transporter (VGAT). These proteins have distinct roles in inhibition: gephyrin is a scaffolding protein that stabilizes inhibitory receptors (i.e., glycine and GABAA receptors) at inhibitory synapses (Tretter et al., 2012; Choii and Ko, 2015; Groeneweg et al., 2018), and VGAT is a transporter present in GABAergic and glycinergic neurons, which is responsible for loading cytoplasmic GABA and glycine into synaptic vesicles and subsequent exocytosis (Juge et al., 2013). As shown in Figures 1C and 1D, none of these proteins changed following training over the 48-h time course.

Significant increase in high-PV-expressing cells in the CA1 hippocampal subregion following infantile training

We then used immunohistochemical analyses to determine in which subregions of the dHPC PV increases following learning. PN17 rats were trained in IA or remained in the home cage (naive controls) and, 48 h later, they were perfused for immunohistochemical staining. Coronal sections of the rat brains sampling the dHPC were immunostained with an anti-PV antibody. Eighteen images (nine per side) per animal were analyzed in the CA1 (n = 3 rats), CA3 (n = 4 rats), and dentate gyrus (DG, n = 4 rats), while 12 images (six per side) were analyzed for the CA2 hippocampal subregion (n = 3 rats). The number of PV+ cells in each hippocampal subregion was measured by PV+ cell body count normalized

against total area quantified (CA1, 200,000 μm^2; CA2, 80,000 μm^2; CA3, 300,000 μm^2; DG, 300,000 μm^2). The cell body PV protein levels were measured by quantifying cell body intensity in arbitrary units (a.u.) of each PV+ cell present in the total area of analysis and plotting individual PV intensity values in a cumulative distribution plot, followed by a Kolmogorov-Smirnov test.

As shown in Figure 2A PV cell density (i.e., PV+ cell number per area) did not change with training in any of the hippocampal subregions. Furthermore, despite there being a tendency for PV intensity to increase in the CA3 and DG, these changes did not reach significance. However, PV intensity increased significantly in CA1 (Figure 2B), a subregion known to be critical for the formation, consolidation, and retrieval of contextual fear memories (Izquierdo and Medina, 1997; Lee and Kesner, 2004; Whitlock et al., 2006; Izquierdo et al., 2016). Additionally, to determine whether PVIs were activated in CA1 following learning, we used immunohistochemistry to quantify the number of PV+ cells expressing the immediate-early gene (IEG) c-FOS 24 h after IA training given at PN17. C-FOS is an activity-dependent IEG that is rapidly induced in response to stimuli; hence, it is widely employed as a marker of neuronal activity (Tischmeyer and Grimm 1999; Perrin-Terrin et al., 2016). C-FOS was analyzed at 24 h after IA training because, in infant rats, the IA training-dependent induction of IEG is slow compared with adults and peaks at 24 h after IA training (Bessières et al., 2020). As shown in Figure 2C, compared with controls, training led to a significant increase in c-FOS immunostaining of PV+ cells in the CA1 of infant rats, indicating that PVIs were activated following infantile IA learning.

Previous studies in adult mice reported that PV levels in the soma of PVIs increase at 6 h following contextual fear conditioning learning in the CA3 and CA1 hippocampal subregions and return to baseline by 48 h post training (Donato et al., 2013, 2015; Karunakaran et al., 2016). To measure changes in the PVI soma levels, these authors classified PV neurons into four subclasses according to the intensity of their cell body defined in a.u.; i.e., into low, intermediate-low, intermediate-high, and high PV. Here we employed the same methodology to compare the PV levels at 48 h post training in the CA1 of infant rats trained in IA at PN17 with those of young adult rats trained in IA at PN80. Double-immunostaining analysis with anti-PV and anti-GAD67 antibodies, detecting the cytosolic enzyme GAD67, which catalyzes the synthesis of GABA from glutamate, relative to a predetermined area (200,000 μm^2), confirmed that PV intensity significantly increased 48 h after IA training in infant rats (Figure 3A) but did not change in adult rats (Figure 3B). As with PV, GAD67+ intensity levels in PV+ neurons significantly increased 48 h after IA training in infant rats (Figure 3A) but not in adult rats (Figure 3B). A correlation analysis revealed that individual neuron PV intensity correlated with GAD67 intensity in all animals (infants, Pearson correlation, 0.90; adults, Pearson correlation, 0.91; Figures 3A and 3B). No changes in PV+ and GAD67+ cell density (number of cells per 200,000 μm^2) or the ratio PV+/GAD67+ density were found following training in either infant or adult CA1 (Figures 3A and 3B).

Training at PN17 led to a significant increase in PV intensity within PVI somas in the CA1 of infant rats 48 h after training (Figures 3C, S2). The subdivision of PVIs into four PV intensity subgroups using parameters similar to those described in Donato et al. (2013),

i.e., low PV (0–5,000 a.u.), intermediate-low PV (5,000–10,000 a.u.), intermediate-high PV (10,000–15,000 a.u.), and high PV (≥15,000 a.u.), revealed that, compared with naive controls, rats that underwent infantile training had a significantly increased fraction of high-PV cells (Figures 3C, S2). In contrast, no changes were found within PVI somas of dHPC CA1 analyzed from trained adult rats euthanized 48 h after training (Figure 3D). Collectively, these results indicated that changes in PV intensity at 48 h after IA training differentially occur in the infant dHPC.

PVIs are required for the formation of infantile memory

We then tested whether PVIs in the infant rat hippocampus play an essential role in memory formation. Toward this end, we bilaterally injected, in the dHPCs of infant rats, an adeno-associated virus (AAV) expressing the inhibitory Designer Receptor Exclusively Activated by Designer Drugs (DREADDs) (AAV-hsyn-DIO-hM4Di-mCherry) engineered to express Cre recombinase selectively in PV+ cells (PV-Cre rats: LE-Tg [Pvalb-iCre]2Ottc).

To quantify the rate of viral infection, we calculated the number of cells bearing double fluorescence for mCherry and endogenous PV (PV+/mCherry+) in the whole dHPC (Figure 4A) 1 week after the virus injection. In the whole dHPC hippocampus, the average number of doubly positive PV+/mCherry+ relative to PV+ cell number was 67.1%. Ninety-three percent of mCherry+ cells expressed PV, indicating that the viral expression selectively targeted hippocampal PV+ cells (Figure 4A). To silence PV cell activity, we injected intraperitoneally (i.p.) compound 21 (C21; Thompson et al., 2018; Goutaudier et al., 2020), a ligand that activates the hM4Di receptor, in PN17 rats 30 min before IA training. First, to confirm that C21 injection silenced PV+ cells, we quantified the number of mCherry+ cells expressing c-FOS at 24 h after training, using immunohistochemistry. As shown in Figure 4B, compared with saline injection, C21 led to a significant decrease in c-FOS immunostaining in mCherry+ cells of the dHPC of IA-trained PV-Cre rats, confirming that C21 silenced the activation of PV+ cells. All dHPC subregions were quantified and the whole-dHPC values are reported. To determine whether C21-silencing affected c-FOS expression in CA1 pyramidal neurons, we employed immunohistochemistry to quantify the number of CAMKIIα+ cells expressing c-FOS at 24 h after training in hm4Di expressing PV-Cre rats. As shown in Figure 4C, compared with saline injection, C21 did not change the number of c-FOS/CAMKIIα-expressing cells in dHPC CA1, confirming that PVI neuronal inhibition did not affect c-FOS expression in pyramidal cells. These results are in line with previous studies showing that inhibiting PVIs in CA1 following contextual fear conditioning in rodents does not increase the mean firing rates of pyramidal cells 24 h post training, nor does it lead to hippocampal seizures or ripple incidence alteration (Xia et al., 2017; Ognjanovski et al., 2017). Similarly, Xia et al. (2017) found no change in the excitability of pyramidal cells in *ex vivo* ACC slices following Clozapine N-oxide (CNO)-mediated inhibition of PVIs (Xia et al., 2017).

Next, we assessed the effect of silencing PV+ cells on infantile memory formation. Bilateral injections of AAV-hsyn-DIO-hM4Di-mCherry into the dHPC of PV-Cre and wild-type littermate rats were performed at PN10 (Figures 4D–4F). After a week, to allow for viral expression, the PN17 rats received an i.p. injection of C21 30 min before IA training.

To control for C21 and virus off-target effects, other cohorts of PV-Cre and wild-type littermate rats were injected with the control virus AAV-hsyn-DIO-mCherry (Figure 4F) and underwent the same treatments and behavioral schedule. As shown in Figure 4D, wild-type and PV-Cre rats that received chemogenetic inhibition of PV+ cells via C21 before training had significant memory retention immediately after training (IT), indicating that dHPC PV+ cells are not required for acquisition and short-term memory. However, chemogenetic inhibition of PV+ cells via C21 before training significantly impaired long-term infantile memory formation relative to the normal memory formed in wild-type and PV-Cre rats injected with the control virus (Figures 4E and 4F), as determined by a significant decrease in retention according to the typical memory reinstatement protocol (T3; Figure 4F). We concluded that PV cell activity is required for long-term infantile memory formation. Re-training of these rats upon entering the shock compartment at T3 resulted, however, in significant memory retention, providing evidence that the chemogenetic inhibition of PV+ cells before training did not damage the hippocampus (T4; Figure 4E).

Injection of diazepam in the dHPC of infant rats promotes long-term memory expression

PVIs exert most of their inhibitory influence via somatic GABAA-receptor-containing synapses (Hensch and Bilimoria, 2012), and maturation of PVIs in the visual cortex is necessary for the development and acquisition of adult-like functional abilities, including adult visual acuity (Hensch et al., 1998; Fagiolini and Hensch, 2000; Fagiolini et al., 2004). In fact, the benzodiazepine diazepam, a known GABAA-receptor-positive allosteric modulator, accelerates the maturation of the critical period in the visual cortex (Hensch et al., 1998; Fagiolini and Hensch, 2000; Fagiolini et al., 2004; Hensch, 2005). Diazepam increases GABAA receptor channel conductance in infant hippocampal neurons, as shown by experiments in hippocampal neuronal cultures of 8- to 24-day-old rats and in CA1 pyramidal neurons of PN17 to PN21 rat hippocampal slice preparations (Birnir et al., 2000). Here we tested whether diazepam affects the maturation of memory abilities, i.e., the expression of long-term memory, like that of adult animals.

Bilateral injection of diazepam in the dHPC of rats immediately after IA training at PN17 resulted in significant long-term memory expression at 6 days after training, compared with vehicle (T2; Figure 5A). Two concentrations of diazepam were tested: 1 and 2 μg; both led to long-term memory expression, although a significant effect was only observed for the higher dose. An SO group injected with 2 μg of diazepam excluded that the long-term memory expression was due to the footshock, indicating that the effect was specific for the associative learning. Thus, diazepam, a known GABAA receptor agonist, prevents the rapid forgetting of infantile memories; i.e., it leads to a lasting memory expression, a typical feature of mature memories.

Chemogenetic activation of hippocampal PVIs does not mature infantile memory expression

We then tested whether directly activating PVIs could have an effect similar to that of diazepam (Figures 5B–5F). To this end, we bilaterally injected an AAV expressing the excitatory DREADD receptor (AAV-hsyn-DIO-hM3dq-mCherry) into the dHPC of PV-Cre rats at PN10 (PV-Cre rats: LE-Tg(Pvalb-iCre)2Ottc) and let the virus express for 1 week.

The rate of infection was assessed 1 week following virus injection, at PN17, by quantifying the number of PV+/mCherry+ cells in the dHPC (Figure 5B). We found that 63.2% of endogenous PV+ cells were also mCherry+ and that 93.9% of mCherry+ cells also expressed PV, confirming that the viral infection specifically targeted PV+ cells (Figure 5B). The effect of PV+ cell direct activation by injecting i.p. 30 min before IA training C21, which activates hM3Dq receptors expressed by PV+ cells, was tested. To confirm that C21 injection led to the activation of hM3Dq, and hence of PVIs, we used immunohistochemistry to quantify the number of mCherry+ cells expressing c-FOS at 90 min after training. C-FOS was analyzed at 90min after IA training because studies have shown that a significant activation of DREADDs receptor-dependent stimulation occurs 90 min after C21 injection (Goutaudier et al., 2020). As shown in Figure 5C, compared with saline, C21 injection resulted in a significant increase of c-FOS+ cells within the mCherry+ cell population, confirming that PVIs were activated by the C21 treatment. All dHPC subregions were quantified and the whole-dHPC values are reported. This chemogenetic PV cell activation did not change PV levels 48 h post injection (Figure S3).

Next, the effects of chemogenetic activation of dHPC PVIs at different time points before or after training on infantile IA memory formation were assessed. Groups of rats were trained in IA at PN17 and received an i.p. injection of C21 either 6 h before training (Figure 5D), 30min before training (Figure 5E), or IT (Figure 5F). At none of these time points of chemogenetic activation of PVIs were we able to detect an effect; in fact, all groups of rats showed the typical rapid memory decay and displayed no memory retention at 1 day (T1) and 7 days (T2) after training. As expected, memory expression was reinstated by behavioral reminders at T3 in both wild-type and PV-Cre rats, proving that training had led to the formation of the typical infantile latent memory trace. We concluded that PVI activation alone is not sufficient to prevent the rapid decay of infantile memory expression.

PVIs are required for the maturation of memory competence elicited by BDNF

BNDF promotes the maturation of PVIs by controlling the assembly and maintenance of PV GABAergic synapses (Huang et al., 1999; Chen et al., 2011; Waterhouse et al., 2012; Takesian and Hensch, 2013; Xenos et al., 2018; Guyon et al., 2021), and disruption of BDNF signaling in PV cells leads to abnormal PVI connectivity, altered firing properties, and learning and memory deficits in mice (Xenos et al., 2018; Guyon et al., 2021). Furthermore, BDNF controls the kinetics of the critical period in the developing visual cortex; in fact, blocking BDNF delays the onset of the critical period, and overexpressing BDNF accelerates the closure of the critical period (Hanover et al., 1999; Huang et al., 1999; Anomal et al., 2013).

Our previous studies on infantile memory showed that BDNF has a similar maturational effect on the functional development of memory: blocking BDNF or its receptor TrkB before infantile learning prevents memory formation, and increasing BDNF at the time of training is sufficient to close the rapid forgetting period in rats (Travaglia et al., 2016a; Travaglia et al., 2018). These data, together with the requirement for an mGluR5-NMDAR subunit switch and mechanisms of synaptic maturation taking place with infantile but not adult

learning, led us to propose that hippocampus-dependent memories undergo a critical period (Alberini and Travaglia 2017).

Here we asked if PVI activity is necessary for the ability of BDNF to accelerate the maturation of memory function; i.e., the ability to be expressed long term similarly to an adult long-term memory. Toward this end, we used chemogenetic inhibition of PVIs on rats treated with BDNF, following the protocol of Travaglia et al. (2016a). We bilaterally injected AAV-hsyn-DIO-hM4Di-mCherry into the dHPC of PV-Cre and wild-type littermate rats at PN10; 1 week later, at PN17, the rats were injected i.p. with C21 30 min before IA training; finally, IT, the rats received a bilateral intrahippocampal injection of BDNF or vehicle solution (1× PBS). In agreement with our previous results (Travaglia et al., 2016a), BDNF-injected wild-type rats had significant and context-specific memory retention at 1 day and 7 days after training (Figure 6A). Chemogenetic inhibition of dHPC PVIs significantly blocked this long-term memory expression in the BDNF-injected PV-Cre rats (Figure 6A). Furthermore, compared with vehicle, BDNF injection did not change PV levels in the dHPC of naive or trained rats (Figure S4), despite, similar to what was found in the time course assessment (Figure 1), there being a trend toward an increase in PV level in trained compared with naive rats.

To control for C21 off-target effects, similar experiments were carried out on PV-Cre and wild-type littermate rats infected with the control virus AAV-hsyn-DIO-mCherry (Figure 6B). These rats, upon BDNF injection, like the wild-type rats, had significant context-specific memory retention at 1 day and 7 days after training (Figure 6B). We concluded that PVI activity is required for the effect of BDNF in promoting memory maturation; i.e., the closure of the infantile critical period of memory.

DISCUSSION

This study shows that the levels of PV significantly increase in the dHPCs of infant rats 48 h following IA learning, with a shift in PV intensity from low to high PV expression in CA1 PVIs. Chemogenetic inhibition of dHPC PVIs revealed that PVI activity is necessary for the formation of long-term, latent infantile memories. Our data also show that the facilitation of GABA's inhibitory effect via diazepam promotes long-term memory expression, and thus, memory maturation. In contrast, direct chemogenetic activation of PVIs is not sufficient to produce the maturation of memory expression. Finally, PVI activity is also required for the ability of BDNF to promote long-term memory expression, and thus, memory development. In sum, our results established a key role of PVIs in the formation and maturation of hippocampus-dependent memory.

As the role of PVIs is a key mechanism of sensory functions critical periods, our data add support to the conclusion that the infant hippocampus, like sensory systems, undergoes a critical period (Alberini and Travaglia 2017; Bessières et al., 2020) during which the hippocampus engages, in addition to differential mechanisms, the critical role of PVIs, to shape memory development and the maturation of the hippocampus-dependent memory system.

Unlike other mechanisms, such as the mGluR5-dependent NMDAR switch, which seem to be selectively recruited for memory formation in the infantile hippocampus (Travaglia et al., 2016a), the critical role of PVIs in memory formation is not restricted to early development but continues to be essential in the matured hippocampus and related memory system. In fact, PVIs play a critical role in long-term memory formation in the hippocampus of adult rodents, where they are recruited in rule consolidation or new information acquisition (Donato et al., 2013, 2015; Ç aliskan et al., 2016; Xia et al., 2017; Ognjanovski et al., 2017). Whether the role of PVIs has distinctive features in the developing hippocampal circuitry, relative to the mature one, remains to be understood. Some difference between infant and adult dHPC PVIs functions is expected, because our results indicate that the regulation of learning-dependent PV levels follows a different kinetics at these two ages, as PV levels increased significantly 48 h post IA learning only in the infant hippocampus. Nevertheless, we cannot exclude that, at earlier or different time points following IA learning, PV levels also change in the dHPC of adult rats. Such an outcome would be in line with previous studies showing that contextual fear conditioning in adult mice increases soma PV intensity in the CA1 and CA3 regions. This increase, however, returned to baseline levels by 48 h post training (Donato et al., 2013, 2015; Karunakaran et al., 2016), similarly to what we found in our experiments with IA. We also cannot exclude that different species and learning paradigms may follow distinct kinetics, and further studies are needed to fully characterize the comparative developmental profiles of learning-dependent PV expression regulation.

Nonetheless, it is known that the infant and adult hippocampi are characterized by distinctive biology (Travaglia et al., 2016b) and show differential kinetic profiles of protein expression following learning (Bessières et al., 2020). For example, in the rat dHPC at baseline, i.e., without a new learning experience, the levels of the IEG products and markers of neuronal activation c-FOS, activity-regulated-cytoskeletal-associated protein (ARC/ARG3.1), and ZIF268, are significantly higher at PN17 compared with PN24 (juvenile age) and PN80 (young adult age) (Travaglia et al., 2016b). Moreover, their significant upregulation evoked by infantile learning is much slower and longer lasting, peaking at 24 h after training. This increase is very slow compared to those of juvenile and adult learning with which the increase peaks around 1–2 h after training, and returns to baseline within a few hours (Bessières et al., 2020). These data imply that, first, there is a higher level of activity in the infant hippocampus relative to the juvenile and adult, and, second, that the cellular activation evoked by infantile learning follows a differential kinetic, which is more prolonged and persistent relative to that of adult learning. Thus, our findings of a differential increase of PV levels at 48 h after IA training in the infant dHPC may be related to the slower and more persistent kinetic of neuronal activation. In line with studies showing that PV levels are modulated by activity, as inhibiting PVIs shifts them to a low PV content while activating PVIs shifts them to a high PV content (Donato et al., 2013, 2015), we suggest that PVI activity is involved in balancing the overall slow and persistent increase in hippocampal activity after infantile learning. In agreement with this idea, some studies reported that PV levels may affect PVI synaptic transmission only if expressed at high levels when they can act as an efficient anti-facilitation factor, thereby modulating neurotransmitter release (Eggermann and Jonas, 2012; Bischop et al., 2012; Hu et al., 2014).

It is also possible that the late, differential increase of PV levels in the infant relative to adult hippocampus may be due to intrinsic features of immature PVIs, which are known to be electrophysiologically distinct from mature PVIs (Okaty et al., 2009; Doischer et al., 2008; Que et al., 2021). PVIs undergo substantial development over the first four postnatal weeks, reflected by a decline in input resistance and an increase in the ability to integrate inputs over smaller time windows, and achieve increasingly higher firing rates (Okaty et al., 2009). Immature PVIs are slower and produce weaker inhibition than mature PVIs because of their lower firing rate (Okaty et al., 2009; Doischer et al., 2008; Que et al., 2021), despite the fact that infantile learning, like adult learning, eventually leads to a switch from low to high PV expression.

The mechanisms by which the increase in PV level in the CA1 subregion contributes to long-term changes underlying the lasting storage of a latent memory are still unknown. Once again, whether similar and/or differential mechanisms underlie the regulation of PV expression in response to learning in the dHPC remains to be investigated. As PV protein is a Ca^{2+} buffer, one pathway to consider that is immediately linked to neuronal plasticity is the activation of calcium calmodulin kinases (CaMKs). A CaMK family member found to regulate PVIs, and consequently long-term memory, is γCaMKII, which is enriched in PVIs and is required for experience-driven strengthening in theta and gamma rhythmicity and long-term memory (He et al., 2021). One other member, γCaMKI, could also be involved as it seems to function specifically within PVIs to drive nuclear translocation, and thus, signaling (Cohen et al., 2016).

Another possible mechanism that should be considered in the regulation of PVI functions and plasticity maturation during infantile brain development is the contribution of perineuronal nets (PNNs), chondroitin sulfate glycosaminoglycan (CS-GAG)-based, net-like structures present within the extracellular matrix that surrounds PV cells and their proximal dendrites. Well-developed PNNs appear to be a necessary component for the termination of developmental critical periods (Gibel-Russo et al., 2022) and their assembly requires PVI activity (Cisneros-Franco and de Villers-Sidani, 2019); thus, an increase in PV levels following infantile learning may be linked to the development of PNNs and therefore to the maturation of circuitry properties (Rupert and Shea 2022).

We also showed that GABA modulation via diazepam treatment of the dHPC promotes memory expression long term, a typical feature of the mature memory. These data again agree with those obtained in the visual system, where diazepam promotes the closure of the critical period (Fagiolini and Hensch 2000), further strengthening our conclusion that the hippocampus, like sensory systems (Hensch et al., 1998; Fagiolini and Hensch 2000; Iwai et al., 2003; Hensch and Stryker, 2004; Hensch, 2005), undergoes a critical period. Despite diazepam promoting memory maturation, we found that the direct activation of dHPC PVIs before or after training at PN17 was not sufficient to prevent infantile forgetting. The reason for this outcome is unclear, and further investigations are needed to understand the distinct contribution of activating GABA modulation versus chemogenetic activation of PVIs. It is possible that PVI activation alone is insufficient to prevent infantile forgetting because PVIs at this age produce lower levels of GABA (Takesian and Hensch, 2013) and their firing properties are still immature, so they may not be able to synchronize

local networks. In agreement with this explanation, several studies have shown that PVI firing properties mature by the third to fourth postnatal week in the primary somatosensory cortex and hippocampus (Okaty et al., 2009; Doischer et al., 2008; Que et al., 2021). Moreover, in the dHPC of PN17 rats, glutamic acid decarboxylase (GAD) isoforms GAD65 and GAD67, which catalyze GABA synthesis, are present at significantly lower levels compared with PN24 and adult rats (Travaglia et al., 2016b). In fact, PVIs' fast-spiking properties are necessary to mediate network dynamics essential for memory formation and storage (Hu et al., 2014; Xia et al., 2017; Ognjanovski et al., 2017), and delayed and asynchronous release of GABA from fast-spiking interneurons reduces their spike reliability and the ability of pyramidal neurons to integrate incoming stimuli into precise firing (Manseau et al., 2010; Volman et al., 2011). Conversely, diazepam as a positive allosteric modulator that increases the chloride flux through GABAA receptors when bound together with endogenous transmitter (Cherubini and Conti, 2001; Hensch, 2005; Takesian and Hensch, 2013) may be sufficient for activating the target mechanisms required for memory maturation and compensating for the poor presynaptic GABA release.

In addition, we showed that in the hippocampus, the ability of BDNF to control the maturation of memory's functional competence requires PVI activity. Specifically, previous studies from our lab showed that in the dHPC, BDNF regulates the kinetics of the infantile forgetting period: blocking BDNF or its receptor TrkB before infantile learning prevents memory formation, and increasing BDNF at the time of training is sufficient to close the rapid forgetting period in rats (Travaglia et al., 2016a). In this study, using chemogenetic inhibition selective for PV neurons, we showed that the effect of BDNF requires PVI activity, despite BDNF treatment not increasing PV levels. Hence, we speculate that BDNF recruits changes in PV neurons evoked by training but does not regulate PV levels. These data are in line with previous studies on the PVI and BDNF role in sensory system critical periods showing that BNDF promotes the maturation of PVIs (Schinder et al., 2000; Zheng et al., 2011; Guyon et al., 2021; Lau et al., 2022), while disrupting BDNF signaling in PV cells alters PVI connectivity and firing properties and causes learning and memory deficits in mice (Huang et al., 1999; Chen et al., 2011; Waterhouse et al., 2012; Takesian and Hensch, 2013; Xenos et al., 2018; Guyon et al., 2021).

In summary, the results of this study establish a key role of dHPC PVIs in the formation and maturation of hippocampus-dependent memory and in BDNF's ability to mature memory competence in infant rats. These findings add support to the conclusion that the infant hippocampus undergoes a critical period (Alberini and Travaglia 2017; Bessières et al., 2020); during this period, the hippocampus engages, in addition to differential mechanisms, the critical role of PVIs, to shape memory development and the maturation of the hippocampus-dependent memory system. We suggest that the role of the critical period of the hippocampus-dependent memory system is to provide windows of high experience-driven plasticity that then close and limit further circuit changes. We speculate that these circuitry maturations occur in the crosstalk between the hippocampus and connected cortical regions, an essential process required for long-term memory in the mature system. We also speculate that while the hippocampus will retain some plasticity for new memory encoding, this encoding will occur on more structured and established circuitry, which would confer schematic representations over which new learning can build memories more rapidly and

efficiently. While sensory systems may have a stricter developmental schema to accomplish their optimal functioning, the hippocampus-dependent memory system is likely to maintain a higher degree of plasticity to provide learning flexibility, hence the ability to adapt to the changing environment.

Our results have important implications for future investigations on the role of inhibitory circuitry and the balance of excitation/inhibition in the development of healthy cognitive functions and their imbalance in neurodevelopmental disorders (Nomura, 2021).

Limitations of the study

One limitation of our study is the lack of electrophysiological readouts of PV cell responses in the infant hippocampus, a question that shall be addressed by future investigations. Moreover, as pointed out in the “Discussion” section, the mechanisms by which PV levels increase following learning and the repercussions of this change on PV+ cell functions and memory formation need to be understood. Our results showed that PV levels in the infant dHPC rise 48 h following learning but not with chemogenetic activation alone. This distinctive outcome could be due to the slower kinetics and selective activation of DREADDs technology relative to behavioral activation. Employing additional activation technology could be investigated, such as optogenetics or pharmacologically selective effector molecules (PSEMs)/pharmacologically selective actuator modules (PSAMs), which more rapidly and/or strongly activate or silence cells directly (Atasoy and Sternson, 2018; Donato et al., 2013); this could help in addressing this point. Finally, while our study showed the critical role of PV+ cell activity in the formation of infantile memory and the ability of BDNF to mature memory competence in infant rats, it did not characterize the mechanisms and role of PV expression regulation following learning. Future studies should be able to address these questions.

STAR★METHODS

RESOURCE AVAILABILITY

Lead contact—Any additional request for resources and reagents should be sent to the lead contact, Cristina Alberini (ca60@nyu.edu).

Materials availability—This study did not generate new unique reagents.

Data and code availability

- Additional requests should be sent to the lead contact, Cristina Alberini (ca60@nyu.edu).
- This paper does not report original code.
- Any additional information required to reanalyze the data reported in this work paper is available from the lead contact upon request.

EXPERIMENTAL MODEL AND SUBJECT DETAILS

Animals—Seventeen-day-old male and female rats were obtained from pregnant Long Evans female rats (Charles River Laboratories). Adult male and female Long-Evans rats weighing 150–250 g (age 2–4 months) were obtained from Envigo. LE-Tg (Pvalb-iCre)20ttc male rats were obtained via the Rat research Resource Center (RRRC #00773), which were generated as described in Wright et al. (2021). Seventeen-day-old male and female LE-Tg (Pvalb-iCre)20ttc rats were obtained by crossing male hemizygous LE-Tg (Pvalb-iCre)20ttc to Long Evans females. Therefore, 50% of offspring contained the Pvalb – iCre allele. Rats were housed in 30.80 cm × 40.60 cm × 22.23 cm plastic cages, containing ALPHA-dri® bedding, under a 12 h light/dark cycle (light on at 07:00 a.m.) with food and water *ad libitum*. All experiments were carried out during the light cycle. The birth date was considered PN0 and the litters were culled to 10–12 animals per litter. Only one male and female per litter was used per experimental condition. For all the experiments, statistical analyses showed no significant difference when comparing males versus female (unpaired two-tailed Student's t-test, $p > 0.05$). Rats were weaned at PN21. All procedures complied with the US National Institute of Health Guide for the Care and Use of Laboratory Animals and were approved by the New York University Animal Care Committees.

METHOD DETAILS

Inhibitory avoidance—Inhibitory avoidance (IA) was carried out as previously described (Travaglia et al., 2016a). The IA chamber (Med Associates Inc., St. Albans, VT) consisted of a rectangular Perspex box divided into a safe compartment and a shock compartment (each 20.3 cm × 15.9 cm × 21.3 cm). The safe compartment was white and illuminated and the shock compartment was black and dark. The apparatus was located in a sound-attenuated, red-illuminated room. During training sessions, each rat was placed in the safe compartment with its head facing away from the door. After 10 s, the door separating the compartments automatically opened, allowing the rat access to the shock compartment. The door closed automatically when the rat entered the shock compartment with all four limbs, and a foot shock (2 s, 1 mA) was administered. Foot shocks were delivered to the grid floor of the shock chamber via a constant current scrambler circuit. Each animal remained in the dark compartment for additional 10 s before it was returned to its home cages until testing for memory retention at designated time points. As controls, we used naive animals (handled and remained in their home cage) and rats exposed to a foot-shock without the IA context experience (shock-only). Shock-only consisted in placing the rat onto the grid of the shock compartment and, immediately after, delivering a foot-shock of the same duration and intensity used in IA training. This protocol does not induce any association between the context and the foot shock. Retention tests were done by placing the rat back in the safe compartment and measuring its latency to enter the dark compartment. Foot shocks were not administered during the retention tests (unless otherwise specified), and testing was terminated at 900 s. During retraining sessions, rats were tested for memory retention and received a foot-shock upon entering into the dark compartment. Locomotor activity was measured in the IA chamber by automatically counting the number of times each rat crossed the invisible infrared light photosensor during training and testing. Reminder foot shocks (RS) were administered in a novel, neutral chamber with transparent walls at

identical duration and intensity to that of training. Context generalization was tested in a new, modified IA box (novel context, NC) with a smooth plastic floor and decorated colorful walls, located in a different experimental room.

Hippocampal cannula implants and injections—On PN15, pups were anesthetized with isoflurane mixed with oxygen. Stainless steel cannulas (26-gauge) were implanted bilaterally in the dHPC (−3.0 mm anterior, 2.2 mm lateral, and −2.3 mm ventral from bregma) through holes drilled in the overlying skull. The cannulas were fixed to the skull with dental cement. After recovery from the surgery, pups were returned to the dam and littermates for a 2-day recovery period prior to experimental manipulations. Hippocampal injections used a 36-gauge needle that extended 1 mm beyond the tip of the guide cannula and was connected via polyethylene tubing to a Hamilton syringe. Injections were delivered using an infusion pump at a rate of 0.1 μL/min to deliver a total volume of 0.3 μL per side over 3 min. The injection needle was left in place for 2 min after injection to allow complete diffusion of the solution. Diazepam (Sigma-Aldrich, cat# 1185008), a GABAA receptor modulator, was dissolved in 50% propylene glycol (Sigma, cat #1576708) and injected at 1 μg or 2 μg per side. Recombinant BDNF (PeproTech, cat# 450-02) was dissolved in 1× PBS and injected at 0.25 μg per side. This dose has been shown to prevent infantile forgetting and rescue memory impairment caused by inhibition of hippocampal protein synthesis and glucocorticoid receptors (Travaglia et al., 2016a; Chen et al., 2012). To verify proper placement of the cannula implants, rats were euthanized at the end of the behavioral experiments, and their brains were frozen in isopentane, sliced in 40μm coronal sections in a −20°C cryostat, and examined under a light microscope for cannula placement. Rats with incorrect placement (5%) were discarded from the study.

Western blot analyses—Rats were euthanized, and their brains were rapidly removed and frozen in isopentane. DHPC punches were obtained with a neuro punch (19 gauge; Fine Science Tools, Foster City, CA) from frozen brains mounted on a cryostat. Samples were homogenized in ice-cold RIPA buffer (50 mM Tris base, 150 mM NaCl, 0.1% SDS, 0.5% Na-deoxycholate, 1% NP-40) with protease and phosphatase inhibitors (0.5 mM PMSF, 2 mM DTT, 1 mM EGTA, 2 mM NaF, 1 μM microcystin, 1 mM benzamidine, 1 mM sodium orthovanadate, and commercial protease and phosphatase inhibitor cocktails (Sigma-Aldrich). Protein concentrations were determined using the Bio-Rad protein assay (Bio-Rad Laboratories, Hercules, CA, USA). Equal amounts of the total protein (20 μg per lane) were resolved on denaturing SDS-PAGE gels and transferred to the Immobilon-FL Transfer membrane (Millipore) by electroblotting. Membranes were dried, reactivated in methanol, washed with water, and then blocked in TBS containing 5% (wt) milk for 1 h at room temperature. Membranes were then incubated with primary antibody overnight at 4°C in the buffer recommended by the manufacturer. The following antibodies were used at the indicated dilutions: Anti-parvalbumin (1:1000, Abcam; cat# ab11427), anti-VGAT (1:1000, Synaptic Systems, cat# 131002), anti-Gephyrin (1:1000, Synaptic Systems, cat# 147111). The membranes were then washed with TBS containing 0.2% Tween 20 (TBST) and incubated with species-appropriate fluorescently conjugated secondary antibody (goat anti-mouse IRDye 680LT (1:10,000), goat anti-rabbit IRDye 800CW (1:10,000) or IRDye streptavidin 800CW (1:10,000) from LI-COR Bioscience (Lincoln, NE, USA)) for 1 h at

room temperature. Membranes were washed again in TBST and scanned using the Odyssey Infrared Imaging system (Li-Cor Bioscience). Data were quantified using pixel intensities with the Odyssey software (Li-Cor) according to the protocols of the manufacturer. Actin (1:20,000, Santa Cruz Biotechnology, Dallas, TX, USA; cat# sc-47778) was used as a loading control for all blots.

Viral and compound 21 (C21) injections—At PN10, wildtype and LE-Tg (Pvalb-iCre)20ttc male and female pups were anesthetized with isoflurane mixed with oxygen. The skull was exposed and holes were drilled in the skull bilaterally above the dHPC. A Hamilton syringe with a 33-gauge needle mounted onto a nanopump (KD Scientific, Holliston, MA) was stereotactically inserted into the dHPC (2.3 mm posterior to bregma, 2.0 mm lateral from midline and 2.8 mm ventral). AAV9/hSyn-DIO-hM4Di-mCherry, AAV9/hSyn-DIO-hM3Dq-mCherry, or AAV9/hsyn-DIO-mCherry (2.3×10^{13} genomic copies/mL, 1 μL per side; Addgene) was microinjected at a rate of 0.2 μL/min. The needle was left in place an additional 6 min following microinjection to ensure complete diffusion of the AAV and then slowly retracted. The scalp was sutured. After recovery from the surgery, pups were returned to the dam and littermates for a 7-day recovery period prior to experimental manipulations. C21 (HelloBio, cat# HB6124) was dissolved in PBS pH 7.4 and 0.5mg/kg injected intraperitoneally, 6 h prior to, 30 min prior to, or immediately after experimental manipulations. This dosage of C21 is known to activate both DREADD (hM4di/hM3dq) receptors and does not cause any off-target effects (Thompson et al., 2018; Jendryka et al., 2019; Goutaudier et al., 2020). After behavioral experiments, the rats were anesthetized with an *i.p.* injection of 750 mg/kg chloral hydrate and transcardially perfused with 4% paraformaldehyde in PBS pH 7.4, and their brains were postfixed in this solution overnight at 4°C, followed by PBS pH 7.4 with 30% sucrose for at least 48 h. We collected 35-μm brain sections by cryosection. The sections were then incubated with the blocking solution (PBS pH 7.4 with 0.25% Triton X-100, 4% normal goat serum, 1% BSA) for 2 h at room temperature. Then, stainings were performed diluted in the blocking solution for 48 h at 4°C: rabbit anti-parvalbumin (1:10,000, Abcam, cat#ab11427) or rabbit anti-cFos antibodies (1:500, Cell Signaling Technology; mab#2250). Subsequently, the brain sections were stained with goat anti-rabbit Alexa Fluor 488 (1:800, Invitrogen, cat# A11029) for 2 h at room temperature and mounted with Prolong Diamond antifade mountant with DAPI (Invitrogen, cat# P36962). Images were collected by an Olympus VS120 virtual slide microscope (Olympus, Tokyo, Japan) and Leica SP8 confocal microscope (Leica Microsystems, Wetzlar, Germany) under nonsaturating conditions. Quantification was performed using ImageJ software (US National Institutes of Health) by experimenters blind to the experimental conditions. All images of an experiment were processed using the same parameters to remove background and outlier noise. Regions of interest (ROIs) were manually drawn around mCherry, parvalbumin, or cFos expressing cells by an experimenter blind to treatment conditions, and ROIs were then used as masks to overlay and quantify parvalbumin/mcherry or mCherry/cFos colocalization in the exact same location.

Immunohistochemical staining—Rats were anesthetized with an *i.p.* injection of 750 mg/kg chloral hydrate and transcardially perfused with 4% paraformaldehyde in PBS pH 7.4, and their brains were postfixed in this solution overnight at 4°C, followed by

PBS pH 7.4 with 30% sucrose for at least 48 h. We collected 35-μm brain sections by cryosection for free-floating immunofluorescent staining. The sections were then incubated with the blocking solution (PBS pH 7.4 with 0.25% Triton X-100, 4% normal goat serum, 1% BSA) for 2 h at room temperature. Then, double-stainings were performed diluted in the blocking solution for 48 h at 4°C: (1) rabbit anti-parvalbumin (1:10,000, Abcam, cat#ab11427) and mouse anti-gad67 antibodies (1:2000, EMD Millipore; cat# MAB5406); rabbit anti-cFOS (1:500, Cell Signaling Technology; mab#2250) and mouse anti-CAMKIIα (1:300, Millipore, 05-532) or mouse anti-parvalbumin (1:2000, EMD Millipore, MAB1572). Subsequently, the brain sections were stained with goat anti-rabbit Alexa Fluor 647 antibody (1:800, Invitrogen, cat# A-21236) and goat anti-mouse Alexa Fluor 488 (1:800, Invitrogen, cat# A11029) for 2 h at room temperature and mounted with Prolong Diamond antifade mountant with DAPI. Three sections around bregma −2.64mm, 3.24mm and −3.48mm, representing rostral, medial, and caudal dHPC, were used for each set of staining. Three images per side of the dHPC per bregma for each animal (18 images/subregion/animal) were captured by a Leica SP8 confocal microscope at 20x magnification. Quantification was performed using ImageJ software (US National Institutes of Health) by experimenters blind to the experimental conditions. Briefly, all images of an experiment were processed using the same parameters to remove background and outlier noise. Regions of interest (ROIs) were manually drawn around GAD67+ and parvalbumin+ expressing cells by an experimenter blind to treatment conditions, and ROIs were then used as masks to overlay and quantify parvalbumin+ and GAD67+ expression in the exact same location. The numbers of parvalbumin-positive neurons were normalized by area and the number of parvalbumin+ or GAD67+ cells in the area quantified. Parvalbumin cell intensity ranges were established as previously described (Donato et al., 2013). Parvalbumin cells were classified into four intensity groups as follows: low PV, 0–5000 au; intermediate low-PV, 5000–10,000 au; intermediate high-PV, 10,000–15,000 au; high-PV, >15,000 au. PV+ cell intensity levels were normalized against PV+ cell count/area and plotted in a cumulative probability graph, and subsequently, a Kolmogorov-Smirnov test was performed to compare between naive and trained groups.

QUANTIFICATION AND STATISTICAL ANALYSES

Data were analyzed with Prism 8 (GraphPad Software Inc.). No statistical methods were used to predetermine sample sizes, but our sample sizes are similar to those generally employed in the field. No randomization was used to collect the data. Statistical analyses were designed using the assumption of normal distribution and similar variance among groups, but this was not formally tested. The data were analyzed by one- or two-way analysis of variance (ANOVA) followed by post hoc tests. One-way ANOVA followed by Tukey's post hoc test was performed when comparing the groups for which a pairwise post hoc analysis of each group was required. One-way ANOVA followed by Dunnett's post hoc test was used when each group was compared with a single control group. One-way ANOVA followed by Sidak's post hoc test was used when each group was compared with two control groups. Two-way ANOVA followed by Sidak's post hoc tests was used when two factors were compared (e.g., treatment and testing). Non-parametric data were analyzed by a Kolmorogov-Smirnov test. For paired comparisons, Student's t test was used. In all the experiments, both PN17 and adult females and males were included and analyzed as a single

group, because statistical analyses of separate sex groups (n = 4–6) yielded no significant difference (unpaired two-tailed Student's t test, $p > 0.05$). All analyses were two-tailed. The results were considered significant at $p < 0.05$. All of the statistical details of experiments can be found in Table S1.

Supplementary Material

Refer to Web version on PubMed Central for supplementary material.

ACKNOWLEDGMENTS

We thank Alessio Travaglia for technical help with preliminary experiments. We thank Camille Casino for proofreading the manuscript. The work reported in this manuscript was supported by the Dana Foundation, R37 MH065635 and R01 HD103641 to C.M.A., T32-MH019524-27 and T32-NS-86750-5 to J.M., and T32AG052909 to E.C. The LE-Tg (Pvalb-iCre)2Ottc rats (RRRC: 00773) were provided by NIDA IRP Transgenic Rat Project. The graphical abstract and the experimental schemes in Figures 4, 5, 6, S4, and S5 were created with BioRender.com.

INCLUSION AND DIVERSITY

We support inclusive, diverse, and equitable conduct of research.

REFERENCES

Alberini CM, and Travaglia A (2017). Infantile amnesia: a critical period of learning to learn and remember. J. Neurosci. 37 (24), 5783–5795. 10.1523/jneurosci.0324-17.2017. [PubMed: 28615475]

Anomal R, de Villers-Sidani E, Merzenich MM, and Panizzutti R (2013). Manipulation of BDNF signaling modifies the experience-dependent plasticity induced by pure tone exposure during the critical period in the primary auditory cortex. PLoS One 8 (5), e64208. 10.1371/journal.pone.0064208. [PubMed: 23700463]

Atasoy D, and Sternson SM (2018). Chemogenetic Tools for causal cellular and neuronal biology. Physiol. Rev. 98 (1), 391–418. 10.1152/physrev.00009.2017. [PubMed: 29351511]

Bellone C, and Nicoll RA (2007). Rapid bidirectional switching of synaptic NMDA receptors. Neuron 55 (5), 779–785. 10.1016/j.neuron.2007.07.035. [PubMed: 17785184]

Bessières B, Travaglia A, Mowery TM, Zhang X, and Alberini CM (2020). Early life experiences selectively mature learning and memory abilities. Nat. Commun. 11 (1), 628. 10.1038/s41467-020-14461-3. [PubMed: 32005863]

Birnir B, Eghbali M, Everitt AB, and Gage PW (2000). Bicuculline, pentobarbital and diazepam modulate spontaneous GABA(A) channels in rat hippocampal neurons. Br. J. Pharmacol. 131 (4), 695–704. 10.1038/sj.bjp.0703621. [PubMed: 11030718]

Bischop DP, Orduz D, Lambot L, Schiffmann SN, and Gall D (2012). Control of neuronal excitability by calcium binding proteins: a new mathematical model for striatal fast-spiking interneurons. Frontiers in molecular neuroscience 5, 78. 10.3389/fnmol.2012.00078. [PubMed: 22787441]

Bozzi Y, Pizzorusso T, Cremisi F, Rossi FM, Barsacchi G, and Maffei L (1995). Monocular deprivation decreases the expression display (Barco CCID 7751, Belgium) suitably linearized by gamma of messenger RNA for brain-derived neurotrophic factor in the rat correction visual cortex. Neuroscience 69, 1133–1144. 10.1016/s0306-4522(98)00463-1. [PubMed: 8848102]

Çaliskan G, Müller I, Semtner M, Winkelmann A, Raza AS, Hollnagel JO, Rösler A, Heinemann U, Stork O, and Meier JC (2016). Identification of parvalbumin interneurons as cellular substrate of fear memory persistence. Cereb. Cortex 26 (5), 2325–2340, May. 10.1093/cercor/bhw001. [PubMed: 26908632]

Campbell BA, and Spear NE (1972). Ontogeny of memory. Psychol. Rev. 79 (3), 215–236. 10.1037/h0032690. [PubMed: 4341445]

Carmignoto G, and Vicini S (1992). Activity-dependent decrease in NMDA receptor responses during development of the visual cortex. Science 258 (5084), 1007–1011. 10.1126/science.1279803. [PubMed: 1279803]

Cisneros-Franco JM, and de Villers-Sidani É (2019). Reactivation of critical period plasticity in adult auditory cortex through chemogenetic silencing of parvalbumin-positive interneurons. Proc. Natl. Acad. Sci. USA 116 (52), 26329–26331. 10.1073/pnas.1913227117. [PubMed: 31843881]

Chen AI, Nguyen CN, Copenhagen DR, Badurek S, Minichiello L, Ranscht B, and Reichardt LF (2011). TrkB (tropomyosin-related kinase B) controls the assembly and maintenance of GABAergic synapses in the cerebellar cortex. J. Neurosci. 31 (8), 2769–2780, Feb 23. 10.1523/JNEUROSCI.4991-10.2011. [PubMed: 21414899]

Chen DY, Bambah-Mukku D, Pollonini G, and Alberini CM (2012). Glucocorticoid receptors recruit the CaMKIIα-BDNF-CREB pathways to mediate memory consolidation. Nat. Neurosci. 15 (12), 1707–1714. 10.1038/nn.3266. [PubMed: 23160045]

Cherubini E, and Conti F (2001). Generating diversity at GABAergic synapses. Trends in neurosciences 24, 155–162. 10.1016/s0166-2236(00)01724-0. [PubMed: 11182455]

Choii G, and Ko J (2015). Gephyrin: a central GABAergic synapse organizer. Exp. Mol. Med. 47, e158. 10.1038/emm.2015.5. [PubMed: 25882190]

Cohen SM, Ma H, Kuchibhotla KV, Watson BO, Buzsáki G, Froemke RC, and Tsien RW (2016). Excitation-transcription coupling in parvalbumin-positive interneurons employs a novel CaM kinase-dependent pathway distinct from excitatory neurons. Neuron 90 (2), 292–307. 10.1016/j.neuron.2016.03.001. [PubMed: 27041500]

Condé F, Lund JS, and Lewis DA (1996). The hierarchical development of monkey visual cortical regions as revealed by the maturation of parvalbumin-immunoreactive neurons. Dev. Brain Res. 96 (1–2), 261–276, Oct 23. 10.1016/0165-3806(96)00126-5. [PubMed: 8922688]

de Lecea L, del Río JA, and Soriano E (1995). Developmental expression of parvalbumin mRNA in the cerebral cortex and hippocampus of the rat. Brain Res. Mol. Brain Res. 32 (1), 1–13. 10.1016/0169-328x(95)00056-x. [PubMed: 7494447]

Doischer D, Hosp JA, Yanagawa Y, Obata K, Jonas P, Vida I, and Bartos M (2008). Postnatal differentiation of basket cells from slow to fast signaling devices. J. Neurosci. 28 (48), 12956–12968, Nov 26. 10.1523/JNEUROSCI.2890-08.2008. [PubMed: 19036989]

Donato F, Chowdhury A, Lahr M, and Caroni P (2015). Early- and late-born parvalbumin basket cell subpopulations exhibiting distinct regulation and roles in learning. Neuron 85 (4), 770–786. 10.1016/j.neuron.2015.01.011. [PubMed: 25695271]

Donato F, Rompani SB, and Caroni P (2013). Parvalbumin-expressing basket-cell network plasticity induced by experience regulates adult learning. Nature 504 (7479), 272–276. 10.1038/nature12866. [PubMed: 24336286]

Eggermann E, and Jonas P (2012). How the 'slow' Ca2+ buffer parvalbumin affects transmitter release in nanodomain-coupling regimes. Nat Neurosci 15, 20–22. 10.1038/nn.3002.

Fagiolini M, Fritschy JM, Löw K, Möhler H, Rudolph U, and Hensch TK (2004). Specific GABAA circuits for visual cortical plasticity. Science 303 (5664), 1681–1683, Mar 12. 10.1126/science.1091032. [PubMed: 15017002]

Fagiolini M, and Hensch TK (2000). Inhibitory threshold for critical-period activation in primary visual cortex. Nature 404 (6774), 183–186. 10.1038/35004582. [PubMed: 10724170]

Gibel-Russo R, Benacom D, and Di Nardo AA (2022). Non-cell-autonomous factors implicated in parvalbumin interneuron maturation and critical periods. Front. Neural Circuits 16, 875873. 10.3389/fncir.2022.875873. [PubMed: 35601531]

Goutaudier R, Coizet V, Carcenac C, and Carnicella S (2020). Compound 21, a two-edged sword with both DREADD-selective and off-target outcomes in rats. PLoS One 15 (9), e0238156. 10.1371/journal.pone.0238156. [PubMed: 32946510]

Groeneweg FL, Trattnig C, Kuhse J, Nawrotzki RA, and Kirsch J (2018). A key regulatory protein of inhibitory synapses and beyond. Histochem. Cell Biol. 150 (5), 489–508, Nov. 10.1007/s00418-018-1725-2. [PubMed: 30264265]

Guskjolen A, Kenney JW, de la Parra J, Yeung BRA, Josselyn SA, and Frankland PW (2018). Recovery of “lost” infant memories in miceJul 23. Curr. Biol. 28 (14), 2283–2290.e3, e3. 10.1016/j.cub.2018.05.059. [PubMed: 29983316]

Guyon N, Zacharias LR, van Lunteren JA, Immenschuh J, Fuzik J, Märtin A, Xuan Y, Zilberter M, Kim H, Meletis K, et al. (2021). Adult trkB signaling in parvalbumin interneurons is essential to prefrontal network dynamicsApr 7. J. Neurosci. 41 (14), 3120–3141, Epub 2021 Feb 16. 10.1523/JNEUROSCI.1848-20.2021. [PubMed: 33593856]

Hanover JL, Huang ZJ, Tonegawa S, and Stryker MP (1999). Brain-derived neurotrophic factor overexpression induces precocious critical period in mouse visual cortex. J. Neurosci. 19, RC40. 10.1523/JNEUROSCI.19-22-j0003.1999. [PubMed: 10559430]

Hartshorn K, Rovee-Collier C, Gerhardstein P, Bhatt RS, Wondoloski TL, Klein P, Gilch J, Wurtzel N, and Campos-de-Carvalho M (1998). The ontogeny of long-term memory over the first year-and-a-half of life. Dev. Psychobiol. 32, 69–89. [PubMed: 9526683]

Hayne H (2004). Infant memory development: implications for childhood amnesia. Dev. Rev. 24, 33–73.

He X, Li J, Zhou G, Yang J, McKenzie S, Li Y, Li W, Yu J, Wang Y, Qu J, et al. (2021). Gating of hippocampal rhythms and memory by synaptic plasticity in inhibitory interneurons. Neuron 109 (6), 1013–1028.e9, e9. 10.1016/j.neuron.2021.01.014. [PubMed: 33548174]

Hensch TK (2005). Critical period plasticity in local cortical circuits. Nat. Rev. Neurosci. 6, 877–888. 10.1038/nrn1787. [PubMed: 16261181]

Hensch TK, and Bilimoria PM (2012). Re-Opening windows: manipulating critical periods for brain development. Cerebrum 2012, 11. [PubMed: 23447797]

Hensch TK, Fagiolini M, Mataga N, Stryker MP, Baekkeskov S, and Kash SF (1998). Local GABA circuit control of experience-dependent plasticity in developing visual cortex. Science 282 (5393), 1504–1508. 10.1126/science.282.5393.1504. [PubMed: 9822384]

Hensch TK, and Stryker MP (2004). Columnar architecture sculpted by GABA circuits in developing cat visual cortex. Science (New York, N.Y.) 303 (5664), 1678–1681. 10.1126/science.1091031. [PubMed: 15017001]

Howes M, Siegel M, and Brown F (1993). Early childhood memories: accuracy and affect. Cognition 47 (2), 95–119. 10.1016/0010-0277(93)90001-c. [PubMed: 8325000]

Hu H, Gan J, and Jonas P (2014). Fast-spiking, parvalbumin^{+} GABAergic interneurons: from cellular design to microcircuit function. Science 345 (6196), 1255263, Aug 1. 10.1126/science.1255263. [PubMed: 25082707]

Huang Z, Kirkwood A, Pizzorusso T, Porciatti V, Morales B, Bear MF, Maffei L, and Tonegawa S (1999). BDNF regulates the maturation of inhibition and the critical period of plasticity in mouse visual cortex. Cell 98 (6), 739–755, Sep 17. 10.1016/s0092-8674(00)81509-3. [PubMed: 10499792]

Iwai Y, Fagiolini M, Obata K, and Hensch TK (2003). Rapid critical period induction by tonic inhibition in visual cortex. J. Neurosci. 23 (17), 6695–6702, Jul 30. 10.1523/JNEUROSCI.23-17-06695.2003. [PubMed: 12890762]

Izquierdo I, Furini CRG, and Myskiw JC (2016). Fear memory. Physiol. Rev. 96 (2), 695–750, Apr. 10.1152/physrev.00018.2015. [PubMed: 26983799]

Izquierdo I, and Medina JH (1997). Memory formation: the sequence of biochemical events in the hippocampus and its connection to activity in other brain structures. Neurobiol. Learn. Mem. 68, 285–316. 10.1006/nlme.1997.3799. [PubMed: 9398590]

Jendryka M, Palchaudhuri M, Ursu D, van der Veen B, Liss B, Kätzel D, Nissen W, and Pekcec A (2019). Pharmacokinetic and pharmacodynamic actions of clozapine-N-oxide, clozapine, and compound 21 in DREADD-based chemogenetics in mice. Sci. Rep. 9, 4522. 10.1038/s41598-019-41088-2. [PubMed: 30872749]

Juge N, Omote H, and Moriyama Y (2013). Vesicular GABA transporter (VGAT) transports β-alanineNov. J. Neurochem. 127 (4), 482–486. 10.1111/jnc.12393. [PubMed: 23919636]

Karunakaran S, Chowdhury A, Donato F, Quairiaux C, Michel CM, and Caroni P (2016). PV plasticity sustained through D1/5 dopamine signaling required for long-term memory consolidation. Nat.

Neurosci. 19, 454–464, Epub 2016 Jan 25. Erratum in: Nat Neurosci. 2018 Sep;21(9):1290. 10.1038/nn.4231. [PubMed: 26807952]

Klausberger T, Roberts JDB, and Somogyi P (2002). Cell type- and input-specific differences in the number and subtypes of synaptic GABA(A) receptors in the hippocampus. J. Neurosci. 22 (7), 2513–2521, Apr 1. 10.1523/JNEUROSCI.22-07-02513.2002. [PubMed: 11923416]

Lau CG, Zhang H, and Murthy VN (2022). Deletion of TrkB in parvalbumin interneurons alters cortical neural dynamics. J. Cell. Physiol. 237 (1), 949–964. 10.1002/jcp.30571. [PubMed: 34491578]

Lee I, and Kesner RP (2004). Differential contributions of dorsal hippocampal subregions to memory acquisition and retrieval in contextual fear-conditioning. Hippocampus 14 (3), 301–310. 10.1002/hipo.10177. [PubMed: 15132429]

Li S, Callaghan BL, and Richardson R (2014). Infantile amnesia: forgotten but not gone. Learn. Mem. 21 (3), 135–139, Mar. 10.1101/lm.031096.113. [PubMed: 24532837]

Manseau F, Marinelli S, Méndez P, Schwaller B, Prince DA, Huguenard JR, and Bacci A (2010). Desynchronization of neocortical networks by asynchronous release of GABA at autaptic and synaptic contacts from fast-spiking interneurons. PLoS Biol. 8 (9), e1000492, Sep 28. 10.1371/journal.pbio.1000492. [PubMed: 20927409]

Mullally SL, and Maguire EA (2014). Learning to remember: the early ontogeny of episodic memory. Dev. Cogn. Neurosci. 9, 12–29. 10.1016/j.dcn.2013.12.006. [PubMed: 24480487]

Nadel L, and Zola-Morgan S (1984). Infantile amnesia. In Infant Memory (Boston, MA: Springer), pp. 145–172.

Nomura T (2021). Interneuron dysfunction and inhibitory deficits in autism and fragile X syndrome. Cells 10 (10), 2610. 10.3390/cells10102610. [PubMed: 34685590]

Ognjanovski N, Schaeffer S, Wu J, Mofakham S, Maruyama D, Zochowski M, and Aton SJ (2017). Parvalbumin-expressing interneurons coordinate hippocampal network dynamics required for memory consolidation. Nat. Commun. 8, 15039. 10.1038/ncomms15039. [PubMed: 28382952]

Okaty BW, Miller MN, Sugino K, Hempel CM, and Nelson SB (2009). Transcriptional and electrophysiological maturation of neocortical fast-spiking GABAergic interneurons. The Journal of neuroscience : the official journal of the Society for Neuroscience 29, 7040–7052. 10.1523/JNEUROSCI.0105-09.2009.

Perrin-Terrin AS, Jeton F, Pichon A, Frugière A, Richalet JP, Bodineau L, and Voituron N (2016). The c-FOS protein immunohistological detection: a useful tool as a marker of central pathways involved in specific physiological responses in vivo and ex vivo. J. Vis. Exp. (110), 53613, Apr 25. 10.3791/53613. [PubMed: 27167092]

Peterson C, Grant VV, and Boland LD (2005). Childhood amnesia in children and adolescents: their earliest memories. Memory 13 (6), 622–637. 10.1080/09658210444000278. [PubMed: 16076676]

Que L, Lukacsovich D, Luo W, and Földy C (2021). Transcriptional and morphological profiling of parvalbumin interneuron subpopulations in the mouse hippocampus. Nat. Commun. 12 (1), 108. 10.1038/s41467-020-20328-4. [PubMed: 33398060]

Quinlan EM, Philpot BD, Huganir RL, and Bear MF (1999). Rapid, experience-dependent expression of synaptic NMDA receptors in visual cortex in vivo. Nat. Neurosci. 2 (4), 352–357. 10.1038/7263. [PubMed: 10204542]

Reh RK, Dias BG, Nelson CA 3rd, Kaufer D, Werker JF, Kolb B, Levine JD, and Hensch TK (2020). Critical period regulation across multiple timescalesSep 22. Proc. Natl. Acad. Sci. USA 117 (38), 23242–23251, Epub 2020 Jun 5. 10.1073/pnas.1820836117. [PubMed: 32503914]

Rovee-Collier C, and Cuevas K (2009). The development of infant memory. In The Development of Memory in Infancy and Childhood, Courage ML and Cowan N, eds. (New York: Psychology).

Rupert DD, and Shea SD (2022). Parvalbumin-positive interneurons regulate cortical sensory plasticity in adulthood and development through shared mechanisms. Front. Neural Circuits 16, 886629. 10.3389/fncir.2022.886629. [PubMed: 35601529]

Schinder AF, Berninger B, and Poo M (2000). Postsynaptic target specificity of neurotrophin-induced presynaptic potentiation. Neuron 25 (1), 151–163. 10.1016/s0896-6273(00)80879-x. [PubMed: 10707980]

Schneider C, Rasband W, and Eliceiri K (2012). NIH Image to ImageJ: 25 years of image analysis. Nat Methods 9, 671–675. 10.1038/nmeth.2089. [PubMed: 22930834]

Seto-Ohshima A, Aoki E, Semba R, Emson PC, and Heizmann CW (1990). Appearance of parvalbumin-specific immunoreactivity in the cerebral cortex and hippocampus of the developing rat and gerbil brain. Histochemistry 94 (6), 579–589. 10.1007/BF00271984. [PubMed: 2279955]

Takesian AE, and Hensch TK (2013). Balancing plasticity/stability across brain development. Prog. Brain Res. 207, 3–34. 10.1016/B978-0-444-63327-9.00001-1. [PubMed: 24309249]

Thompson KJ, Khajehali E, Bradley SJ, Navarrete JS, Huang XP, Slocum S, Jin J, Liu J, Xiong Y, Olsen RHJ, et al. (2018). DREADD agonist 21 is an effective agonist for muscarinic-based DREADDs in vitro and in vivo. ACS Pharmacol. Transl. Sci. 1 (1), 61–72, Sep 14. 10.1021/acsptsci.8b00012. [PubMed: 30868140]

Tischmeyer W, and Grimm R (1999). Activation of immediate early genes and memory formation. Cell. Mol. Life Sci. 55 (4), 564–574, Apr. 10.1007/s000180050315. [PubMed: 10357227]

Travaglia A, Bisaz R, Sweet ES, Blitzer RD, and Alberini CM (2016a). Infantile amnesia reflects a developmental critical period for hippocampal learning. Nat. Neurosci. 19, 1225–1233. 10.1038/nn.4348. [PubMed: 27428652]

Travaglia A, Bisaz R, Cruz E, and Alberini CM (2016b). Developmental changes in plasticity, synaptic, glia and connectivity protein levels in rat dorsal hippocampus. Neurobiol. Learn. Mem. 135, 125–138. 10.1016/j.nlm.2016.08.005. [PubMed: 27523749]

Travaglia A, Steinmetz AB, Miranda JM, and Alberini CM (2018). Mechanisms of critical period in the hippocampus underlie object location learning and memory in infant rats. Learning & Memory 25, 176–182. 10.1101/lm.046946.117. [PubMed: 29545389]

Tretter V, Mukherjee J, Maric HM, Schindelin H, Sieghart W, and Moss SJ (2012). Gephyrin, the enigmatic organizer at GABAergic synapses. Front. Cell. Neurosci. 6, 23. 10.3389/fncel.2012.00023. [PubMed: 22615685]

Volman V, Behrens MM, and Sejnowski TJ (2011). Downregulation of parvalbumin at cortical GABA synapses reduces network gamma oscillatory activity. J. Neurosci. 31 (49), 18137–18148. 10.1523/JNEUROSCI.3041-11.2011. [PubMed: 22159125]

Waterhouse EG, An JJ, Orefice LL, Baydyuk M, Liao GY, Zheng K, Lu B, and Xu B (2012). BDNF promotes differentiation and maturation of adult-born neurons through GABAergic transmission. J. Neurosci. 32, 14318–14330, 41. 10.1523/JNEUROSCI.0709-12.2012. [PubMed: 23055503]

Whitlock JR, Heynen AJ, Shuler MG, and Bear MF (2006). Learning induces long-term potentiation in the hippocampus. Science 313, 1093–1097. 10.1126/science.1128134. [PubMed: 16931756]

Wright AM, Zapata A, Hoffman AF, Necarsulmer JC, Coke LM, Svarcbahs R, Richie CT, Pickel J, Hope BT, Harvey BK, and Lupica CR (2021). Effects of withdrawal from cocaine self-administration on rat orbitofrontal cortex parvalbumin neurons expressing Cre recombinase: sex-dependent changes in neuronal function and unaltered serotonin signaling. eNeuro 8 (4), ENEURO.0017, 21.2021. 10.1523/ENEURO.0017-21.2021.

Xenos D, Kamceva M, Tomasi S, Cardin JA, Schwartz ML, and Vaccarino FM (2018). Loss of TrkB signaling in parvalbumin-expressing basket cells results in network activity disruption and abnormal behavior. Cereb. Cortex 28 (10), 3399–3413, Oct 1. 10.1093/cercor/bhx173. [PubMed: 28968898]

Xia F, Richards BA, Tran MM, Josselyn SA, Takehara-Nishiuchi K, and Frankland PW (2017). Parvalbumin-positive interneurons mediate neocortical-hippocampal interactions that are necessary for memory consolidation. Elife 6, e27868, Sep 29. 10.7554/eLife.27868. [PubMed: 28960176]

Zheng K, An JJ, Yang F, Xu W, Xu ZQD, Wu J, Hökfelt TGM, Fisahn A, Xu B, and Lu B (2011). TrkB signaling in parvalbumin-positive interneurons is critical for gamma-band network synchronization in hippocampus. Proc. Natl. Acad. Sci. USA 108 (41), 17201–17206. 10.1073/pnas.1114241108. [PubMed: 21949401]

Highlights

- Hippocampal PV interneurons (PVIs) are required for long-term memory in infant rats
- Infantile learning significantly increases levels of PV in the CA1
- Diazepam or BDNF administration in the hippocampus promotes memory maturation
- BDNF-dependent memory maturation requires PVIs

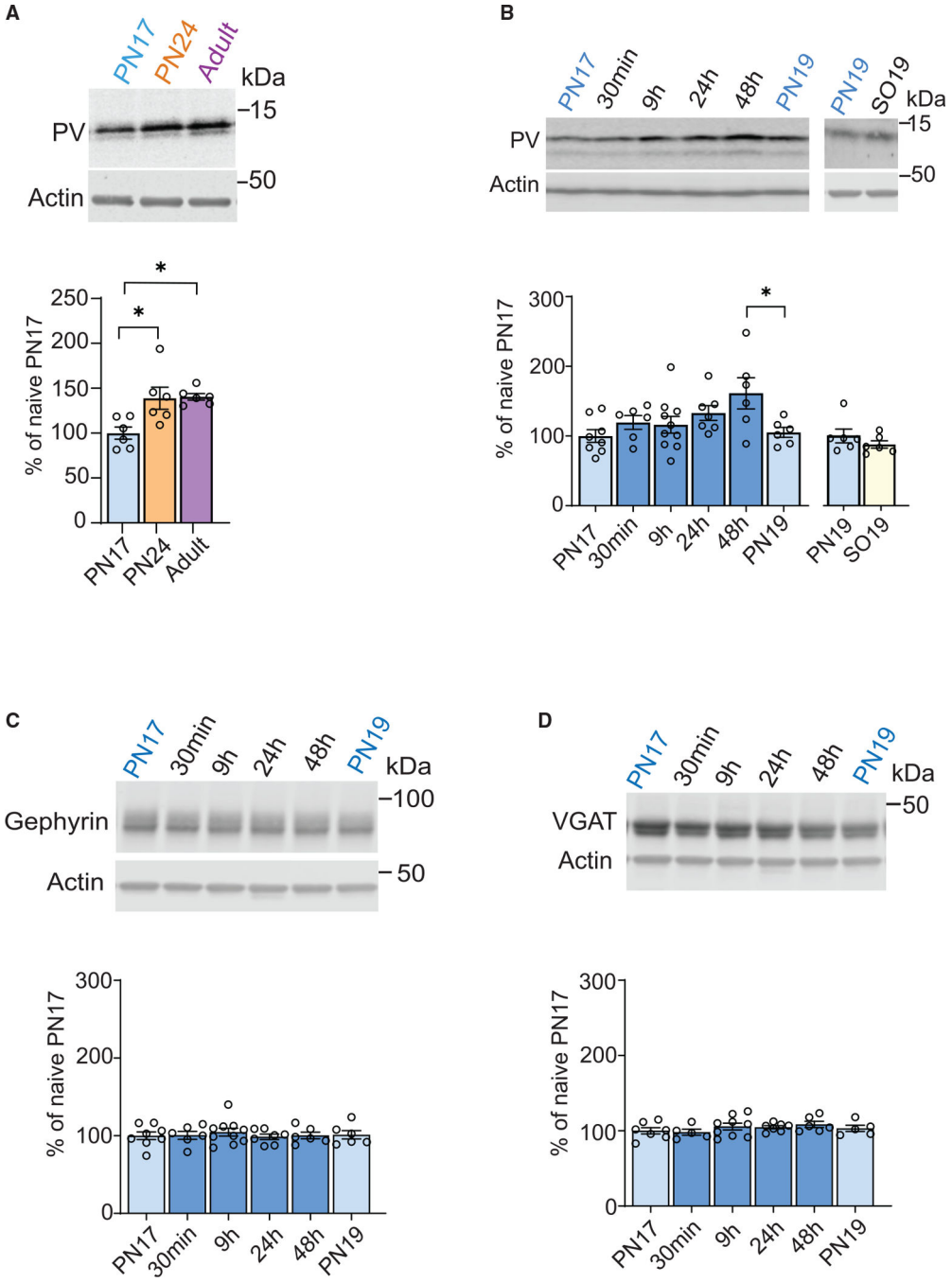

Figure 1. Infantile learning leads to a significant increase in the level of PV

(A) Examples and densitometric western blot analyses of dHPC extracts obtained from rats euthanized at PN17, PN24, or PN80 (n = 6, 6, 6 rats, respectively). Data are expressed as mean percentage ± SEM of PN17 naive rats (one-way ANOVA followed by Dunnett's multiple comparisons test, *p < 0.05, **p < 0.01, ***p < 0.001.

(B–D) Examples and densitometric western blot analyses of extracts obtained from the dHPC of rats trained in IA at PN17 and euthanized 30 min, 9 h, 24 h, 48 h after training (n = eight, six, 10, six, six rats, respectively) probed for PV, gephyrin, and VGAT. To account

for developmental changes, two groups of naive control rats were used: PN17 (n = 8 rats) and PN19 (n = 6 rats). Data are expressed as mean percentage ± SEM of PN17 naive rats (one-way ANOVA followed by Sidak's multiple comparisons test, *p < 0.05, **p < 0.01). (B), Right: densitometric western blot analyses of dHPC extracts obtained from rats that received shock-only (SO) protocol at PN17 and were euthanized 48 h later and were compared with PN19 naive rats (n = 6, 6 rats, respectively). Data are expressed as mean percentage ± SEM of PN19 naive rats (two-tailed unpaired Student's t test, *p < 0.05, **p < 0.01, ***p < 0.001). For detailed statistical information, see Table S1.

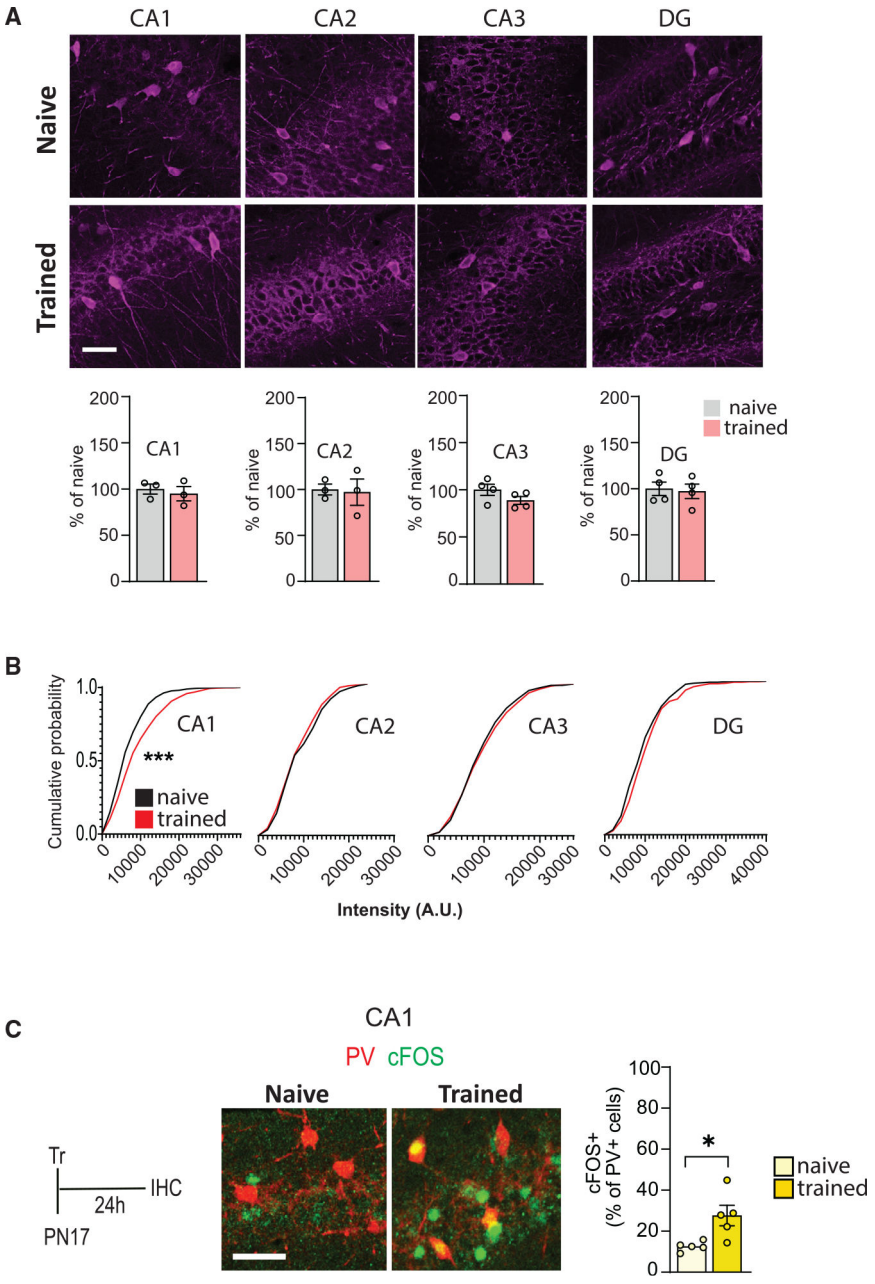

Figure 2. Infantile learning increases PV levels in the CA1 subregion of dHPC

(A) Upper: representative PV images of dHPC CA1, CA2, CA3, and DG subregions obtained from rats untrained (naive) and trained in IA at PN17 and euthanized 48 h after training. Scale bar, 50 μm. Lower: relative quantification of PV+ cell density in CA1, CA2, CA3, and DG in naive and trained rats (CA1 and CA2 n = 3 rats; CA3 and DG n = 4 rats). Data are presented as mean percentage ± SEM of the naive group (two-tailed unpaired Student's t test).

(B) Cumulative probability plots reporting PV+ cell body intensity in arbitrary units (a.u.) using the Kolmogorov-Smirnov test (CA1 naive, 515 cells, three rats; trained, 489 cells,

three rats; CA2, n = 185 cells, three rats; CA3, n = 378 cells, four rats; DG, n = 312 cells, four rats). *p < 0.05, **p < 0.01, ***p < 0.001.

(C) From left: experimental scheme. Representative images of dHPC CA1 showing PV+ cells (red) colocalized with c-FOS+ cells (green) obtained from rats untrained (naive) and trained in IA at PN17 and euthanized 24 h after training. Scale bar, 50 μm; bar graph showing the quantification (percentage) of PV+ cells expressing c-FOS 24 h after IA training in naive and trained rats (n = 5 rats). Data are shown as mean percentage ±SEM of the naive group (two-tailed unpaired Student's t test). *p < 0.05, **p < 0.01, ***p < 0.001. For detailed statistical information, see Table S1.

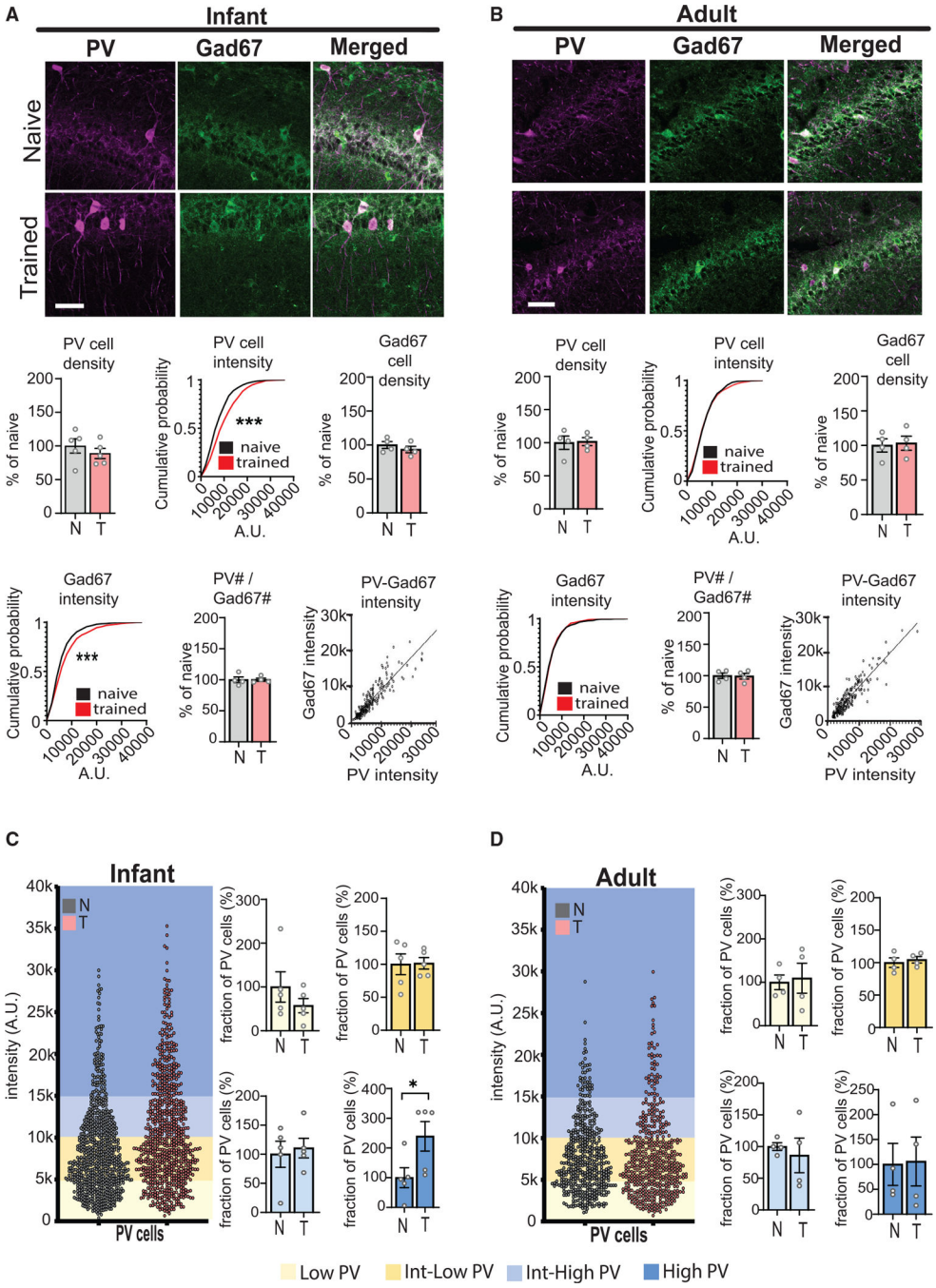

Figure 3. High PV levels increase in the CA1 hippocampal subregion in infant but not adult rats at 48 h post training

(A and B) Upper: representative single and double immunofluorescence staining images of PV+ and GAD67+ cells in CA1 of naive and trained infant and adult rats euthanized at 48 h after training (infant, n = 5 rats per group; adult, n = 4 rats per group). Scale bars, 50 μm. Middle and bottom: bar graphs showing quantification (percentage) of PV+ and GAD67+ cell density in CA1 of infant and adult naive (N) and trained (T) rats. Data are presented as mean percentage ± SEM of the naive group (two-tailed unpaired Student's t test). Cumulative probability plots of PV+ intensity levels according to the Kolmogorov-

Smirnov test (infant naive, 825 cells, five rats; infant trained, 733 cells, five rats; adult naive, 475 cells, four rats; adult trained, 483 cells, four rats) and cumulative probability plots of GAD67+ intensity levels according to the Kolmogorov-Smirnov test (infant naive, 667 cells, four rats; infant trained, 655 cells, four rats; adult naive, 475 cells, four rats; adult trained, 483 cells, four rats). Bottom right of each panel: Pearson correlation of PV and GAD67 intensity level relationship in individual PV neurons, n = 4 rats (50–60 neurons per rat). (C and D) Plots showing the distribution of PV+ intensity according to their values separated as low (0–5,000a.u.), intermediate-low (5,000–10,000a.u.), intermediate-high (10,000–15,000a.u.), and high (≥15,000a.u.) PV. Dots represent intensity values (a.u.) from individual PV+ cell bodies in the CA1 (infant naive, 825 cells, five rats; infant trained, 733 cells, five rats; adult naive, 475 cells, four rats; adult trained: 483 cells, four rats). Bar graphs show the quantification of low, intermediate-low, intermediate-high, and high PV+ cell density in the CA1 of infant (PN17) and adult (PN80) naive and trained rats. Data are shown as mean percentage ± SEM of the naive group (two-tailed unpaired Student's t test, *$p < 0.05$, **$p < 0.01$, ***$p < 0.001$). For detailed statistical information, see Table S1.

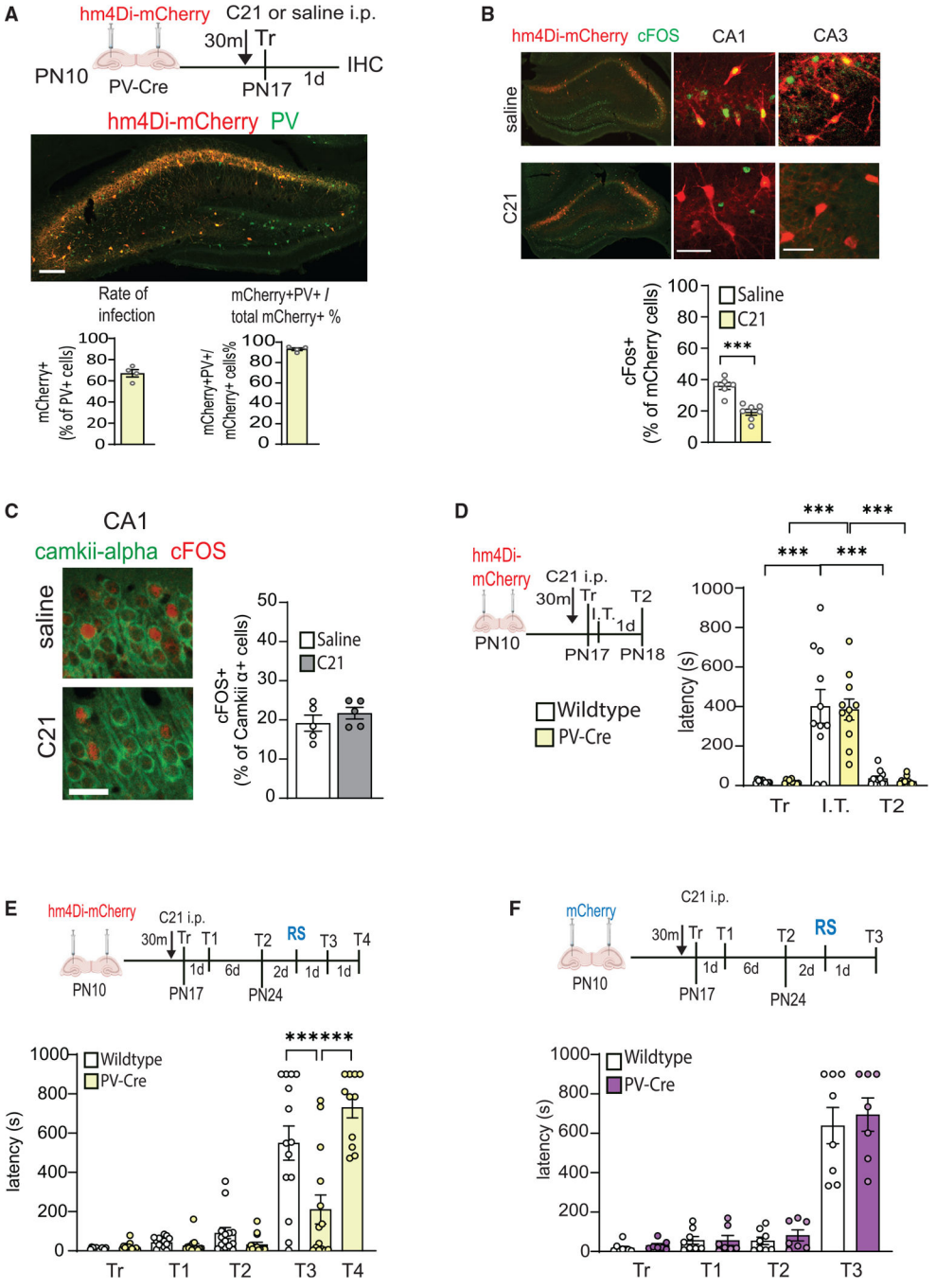

Figure 4. Chemogenetic inhibition of dHPC PVIs at PN17 impairs infantile memory reinstatement

(A) Experimental schedule and representative dHPC image of PV+ cells (green) colocalized to mCherry+ cells (red) in PV-Cre rats injected with AAV9/hsyn-DIO-hM4di-mCherry at PN10 and euthanized 1 week later. Scale bar, 200 μm. PV-Cre rats (saline n = 6 rats; C21 n = 7 rats) expressing hM4Di-mCherry in dHPC PV+ cells were administered C21 (0.5 mg kg^{-1}) or saline i.p. 30 min before undergoing IA training at PN17. Immunohistochemical analyses were carried out 24 h after training. Quantification of the number of PV+ cells relative to the number of mCherry+ cells, expressed as a percentage, revealed the rate

of infection in PV+ cells; the doubly positive PV+ and mCherry+ cells relative to the mCherry+ cell number expressed as a percentage revealed the selectivity of the cells infected (n = 4 rats).

(B) Representative images of the dHPC, and, as examples of higher-magnification images, two panels showing the subregions CA1 (20×) and CA3 (10×) with mCherry+ cells (red) colocalized with c-FOS+ cells (green) in PV-Cre rats expressing AAV9/hsyn-DIO-hM4di-mCherry and injected with C21 (0.5 mg kg^{-1}) or saline i.p. 30 min before IA training at PN17 and euthanized 24 h after training. Scale bars, 50 μm. Percentage of PV+ cells expressing c-FOS 24 h after IA training in saline- and C21-injected PV-Cre rats (saline n = 6 rats; C21 n = 7 rats). Data are shown as mean percentage ± SEM of the saline group (two-tailed unpaired Student's t test). *p < 0.05, **p < 0.01, ***p < 0.001.

(C) Percentage of CAMKIIα+ cells expressing c-FOS 24 h after IA training in saline- and C21-injected PV-Cre rats (saline, n = 5 rats; C21, n = 5 rats). Data are shown as mean percentage ± SEM of the saline group (two-tailed unpaired Student's t test). *p < 0.05, **p < 0.01, ***p < 0.001. Scale bar, 50 μm.

(D) IA short-term memory test in wild-type and PV-Cre rats. Experimental schedule shown above graphs. Rats were bilaterally injected in the dHPC with AAV9/hsyn-DIO-hM4di-mCherry at PN10 and then injected i.p. at PN17 with C21 and 30 min later trained in IA. The rats were tested immediately after training (IT), and 1 day later (T2). IA memory retention is expressed as mean latency ± SEM (in seconds). Two-way ANOVA followed by Sidak's *post hoc* tests for pairwise comparisons (both wild-type and PV-Cre n = 11 rats, *p < 0.05, **p < 0.01, ***p < 0.001).

(E and F) Long-term IA memory test in wild-type and PV-Cre rats. Experimental schedule shown above graphs. Rats were bilaterally injected in the dHPC with AAV9/hsyn-DIO-hM4di-mCherry (E) or AAV9/hsyn-DIO-mCherry (F) at PN10 and then injected i.p. at PN17 with C21 and trained in IA 30 min after injection. The rats were tested 1 day (T1), 7 days (T2), after behavioral reminder (T3), and after re-training (T4). IA memory retention is expressed as mean latency ± SEM (in seconds). Two-way ANOVA followed by Sidak's *post hoc* tests for pairwise comparisons (E, both wild-type and PV-Cre n = 14 rats, *p < 0.05, **p < 0.01, ***p < 0.001; F, wild type n = 8 rats; PV-Cre n = 7 rats, *p < 0.05, **p < 0.01, ***p < 0.001). For detailed statistical information, see Table S1.

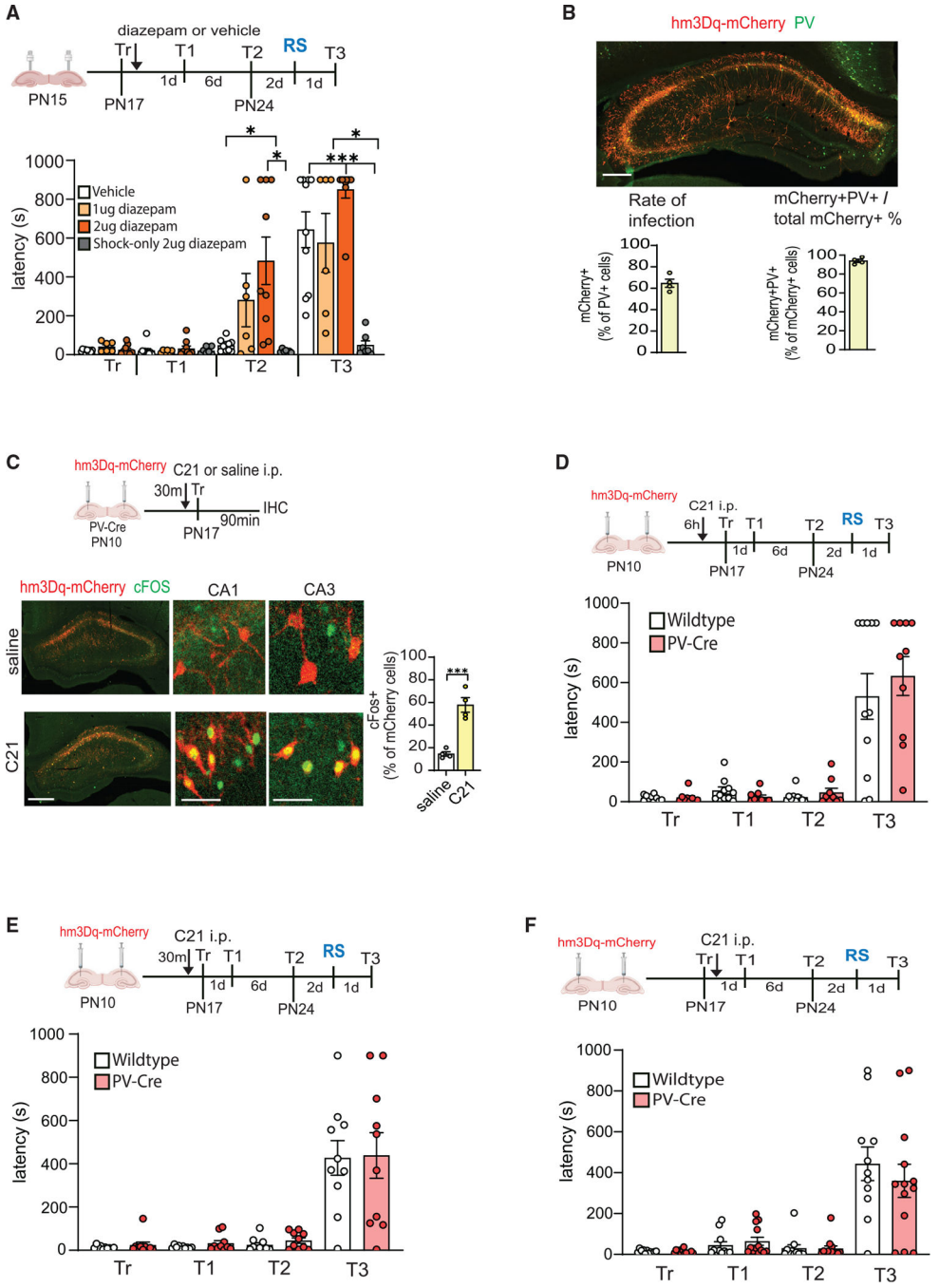

Figure 5. Diazepam in the dHPC matures memory expression, whereas chemogenetic activation of PVIs is not sufficient to prevent the rapid infantile forgetting

(A) Experimental schedule: diazepam or vehicle (arrow) was injected bilaterally into the dHPC of PN17 rats immediately after IA training; the rats were tested 1 day (T1), 7 days (T2) after training, and 1 day after behavioral reminders (T3). Mean latency ± SEM (expressed in seconds). Two-way ANOVA followed by Tukey's *post hoc* tests (vehicle, n = 10 rats; diazepam, 1 μg, n = 7 rats; diazepam 2 μg, n = 10 rats; SO diazepam 2 μg, n = 7 rats; *p < 0.05, **p < 0.01, ***p < 0.001).

(B) Representative dHPC image showing the colocalization of PV+ cells (green) with mCherry+ cells (red) in PV-Cre rats injected with AAV9/hsyn-DIO-hM3dq-mCherry at PN10 and euthanized 1 week later. Scale bar, 200 μm. Bar graphs report the rates of infection and specificity, shown respectively by percentage of doubly stained PV+ mCherry+ relative to PV and PV+ mCherry+ over total mCherry+ (n = 4 rats per group).
(C) Experimental schedule and representative images of the dHPC, and, as examples of higher-magnification images, two panels showing the subregions CA1 and CA3 with c-FOS+ cells (green) colocalized with mCherry+ cells (red) in PV-Cre rats injected with AAV9/hsyn-DIO-hM3dq-mCherry at PN10 and administered C21 (0.5 mg kg^{-1}) or saline i.p. 30 min before IA training at PN17. The rats were euthanized 90 min after training for immunohistochemical analyses. Scale bars, 50 μm. Percentage of PV+ cells expressing c-FOS 90 min after IA training in saline- and C21-injected PV-Cre rats (both saline and C21, n = 4 rats per group). Data are shown as mean percentage ± SEM of the saline group (two-tailed unpaired Student's t test). *p < 0.05, **p < 0.01, ***p < 0.001.
(D–F) IA memory test in wild-type and PV-Cre rats. Experimental schedule shown above graphs. Rats were bilaterally injected in the dHPC with AAV9/hsyn-DIO-hM3dq-mCherry at PN10 and then injected i.p. at PN17 with C21 6 h before (D), 30 min before (E), or immediately after (F) undergoing IA training. The rats were tested 1 day (T1), 7 day (T2), and 1 day after behavioral reminder (T3). IA memory retention is expressed as mean latency ± SEM (in seconds). Two-way ANOVA followed by Sidak's *post hoc* tests for pairwise comparisons (E, both wild-type and PV-Cre n = 10 rats, *p < 0.05, **p < 0.01, ***p < 0.001; F, wild-type n = 11 rats; PV-Cre n = 13 rats, *p < 0.05, **p < 0.01, ***p < 0.001). For detailed statistical information, see Table S1.

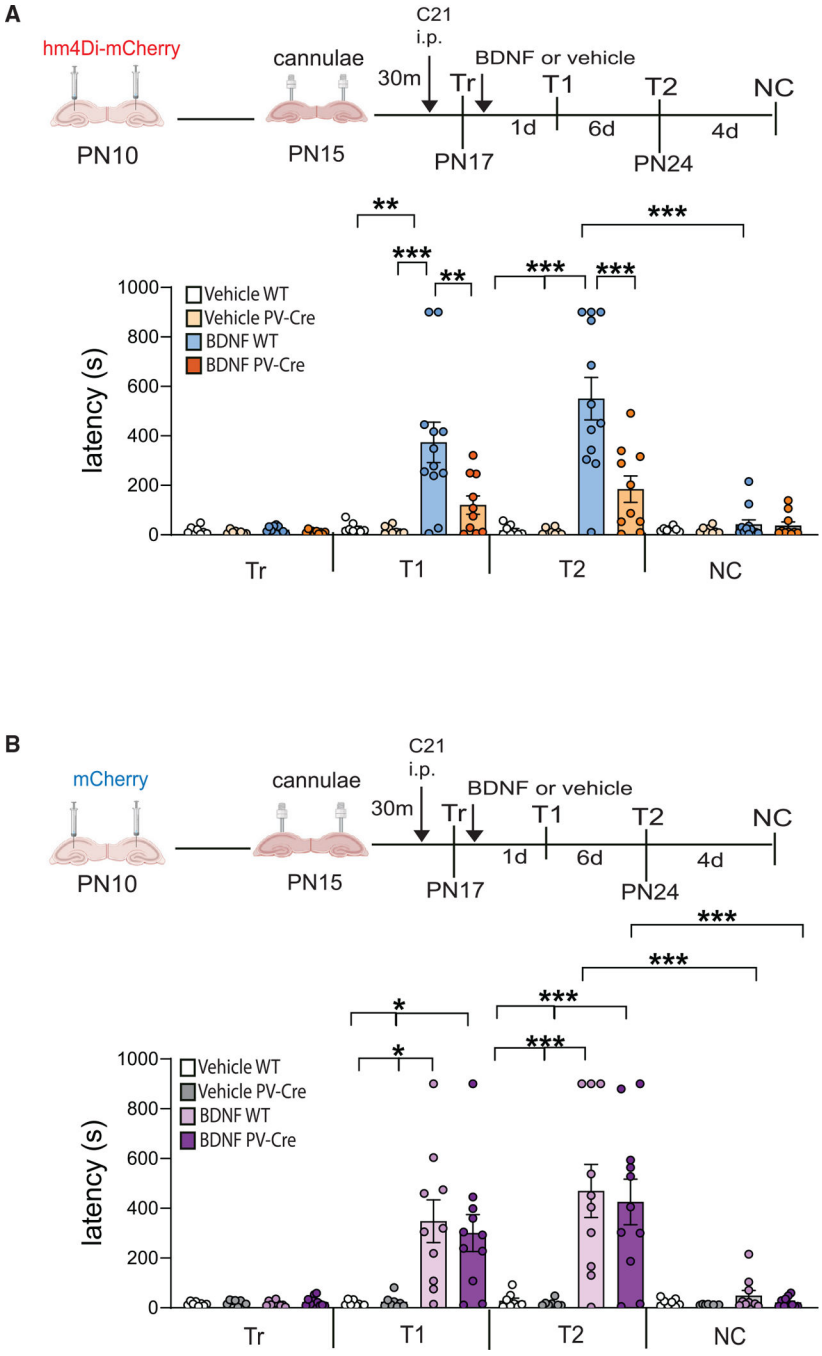

Figure 6. BDNF-induced maturation of hippocampus-dependent memory requires PVI in the dHPC

(A and B) Experimental schedule shown above graphs. Rats were bilaterally injected in the dHPC with AAV9/hsyn-DIO-hM4di-mCherry (A) or AAV9/hsyn-DIO-mCherry (B) at PN10 and then injected i.p. at PN17 with C21 and trained in IA 30 min later. Immediately after, the rats received a bilateral dHPC injection of vehicle or BDNF. The rats were tested 1 day (T1), 7 days (T2), and, 4 days later, in a new context (NC). IA memory retention is expressed as mean latency ± SEM (in seconds). Two-way ANOVA followed by Tukey's *post hoc* tests for pairwise comparisons (A, both wild-type and PV-Cre vehicle n = 8 rats;

wild-type BDNF n = 12 rats; PV-Cre BDNF n = 10 rats, *p < 0.05, **p < 0.01, ***p < 0.001; B, both wild-type and PV-Cre vehicle n = 8 rats; wild-type BDNF n = 10 rats; PV-Cre BDNF n = 11 rats, *p < 0.05, **p < 0.01, ***p < 0.001). For detailed statistical information, see Table S1.

KEY RESOURCES TABLE

REAGENT or RESOURCE	SOURCE	IDENTIFIER
Antibodies		
anti-parvalbumin	Abcam	Cat# ab11427; RRID: AB_298032
anti-parvalbumin	EMD Millipore	Cat# MAB1572; RRID: AB_2174013
anti-GAD67	EMD Millipore	Cat# MAB5406; RRID: AB_2278725
anti-VGAT	Synaptic Systems	Cat# 131002; RRID: AB_887871
anti-Gephyrin	Synaptic Systems	Cat# 147111; RRID: AB_887719
Goat anti-mouse IRdye680LT	LI-Cor Bioscience	Cat# 926-68020; RRID: AB_10706161
Goat anti-rabbitIRdye800CW	LI-Cor Bioscience	Cat# 926-32211; RRID: AB_621843
Actin	Santa Cruz Biotechnology	Cat# sc-47778; RRID: AB_626632
Bacterial and virus strains		
AAV9/hSyn-DIO-hM4Di-mCherry	Addgene, this was a gift from Bryan Roth	Cat# 44362
AAV9/hSyn-DIO-hM3Dq-mCherry	Addgene, this was a gift from Bryan Roth	Cat# 44361
AAV9/hsyn-DIO-mCherry	Addgene, this was a gift from Bryan Roth	Cat# 50459
Chemicals, peptides, and recombinant proteins		
Diazepam	Sigma-Aldrich	Cat# 1185008
BDNF	PeproTech	Cat# 450-02
Propylene glycol	Sigma	Cat #1576708
Compound 21	HelloBio	Cat# HB6124
Experimental models: Organisms/strains		
LE-Tg(Pvalb-iCre)2Ottc	Rat Resource and Research Center	RRRC# 00773
Pregnant Long Evans	Charles Rivers Laboratories	Strain Code: 006
Adult male and female Long Evans	Envigo	Order code: 140
Software and algorithms		
ImageJ	Schneider et al., 2012	https://imagej.nih.gov/ij/